Aging Brain 5 (2024) 100105

Contents lists available at ScienceDirect

Aging Brain

journal homepage: www.elsevier.com/locate/nbas

Age-related differences in structural and resting-state functional brain network organization across the adult lifespan: A cross-sectional study

Maedeh Khalilian [a], Monica N. Toba [a,b], Martine Roussel [a], Sophie Tasseel-Ponche [a,c], Olivier Godefroy [a,b,d], Ardalan Aarabi [a,b,*]

[a] Laboratory of Functional Neuroscience and Pathologies (UR UPJV 4559), University Research Center (CURS), University of Picardy Jules Verne, Amiens, France
[b] Faculty of Medicine, University of Picardy Jules Verne, Amiens, France
[c] Neurological Physical Medicine and Rehabilitation Department, Amiens University Hospital, University of Picardy Jules Verne, Amiens, France
[d] Neurology Department, Amiens University Hospital, Amiens, France

ARTICLE INFO

Keywords:
Brain structural connectivity
Brain functional connectivity
Rich-club organization
Structure–function coupling
Vulnerability analysis
Aging

ABSTRACT

We investigated age-related trends in the topology and hierarchical organization of brain structural and functional networks using diffusion-weighted imaging and resting-state fMRI data from a large cohort of healthy aging adults. At the cross-modal level, we explored age-related patterns in the RC involvement of different functional subsystems using a high-resolution functional parcellation. We further assessed age-related differences in the structure–function coupling as well as the network vulnerability to damage to rich club connectivity.

Regardless of age, the structural and functional brain networks exhibited a rich club organization and small-world topology. In older individuals, we observed reduced integration and segregation within the frontal-occipital regions and the cerebellum along the brain's medial axis. Additionally, functional brain networks displayed decreased integration and increased segregation in the prefrontal, centrotemporal, and occipital regions, and the cerebellum. In older subjects, structural networks also exhibited decreased within-network and increased between-network RC connectivity. Furthermore, both within-network and between-network RC connectivity decreased in functional networks with age. An age-related decline in structure–function coupling was observed within sensory-motor, cognitive, and subcortical networks. The structural network exhibited greater vulnerability to damage to RC connectivity within the language-auditory, visual, and subcortical networks. Similarly, for functional networks, increased vulnerability was observed with damage to RC connectivity in the cerebellum, language-auditory, and sensory-motor networks. Overall, the network vulnerability decreased significantly in subjects older than 70 in both networks. Our findings underscore significant age-related differences in both brain functional and structural RC connectivity, with distinct patterns observed across the adult lifespan.

* Corresponding author at: Laboratory of Functional Neuroscience and Pathologies (UR UPJV 4559), University Research Center (CURS), University of Picardy Jules Verne, Amiens, France.
E-mail address: ardalan.aarabi@u-picardie.fr (A. Aarabi).

https://doi.org/10.1016/j.nbas.2023.100105
Received 11 April 2023; Received in revised form 20 December 2023; Accepted 22 December 2023

Introduction

Advances in brain imaging techniques have allowed assessments of age-related patterns in brain structure and function during normal aging [6,15,85,88]. Morphometric MRI studies have demonstrated reductions in grey/white matter (GM/WM) volumes and GM thickness mainly in prefrontal, parietal and temporal cortices and deep structures [41,64,76,88,97]. Growing evidence, however, suggests that local age-related variations in brain morphology are highly related to gradual alterations in the brain's structural and functional organization.

The emergence of network neuroscience has allowed scientists to better study the topology of whole-brain networks [19,90]. Over the past decade, network-based studies have substantially advanced our understanding of age-related trends in the brain's structural and functional connectivity [13,63,84,114]. For structural connectivity (SC) analysis, a structural network is derived from diffusion magnetic resonance imaging data by fiber tracking or tractography to infer white matter fiber connectivity patterns between brain regions. For functional connectivity (FC) analysis, a functional network is usually derived from resting-state functional MRI (rsfMRI) by inferring statistical independence between brain regions through correlation analysis. The whole-brain functional connectivity network can be decomposed into so-called resting-state networks (RSN) including default mode (DMN), executive control, attention (ATN), salience, sensorimotor and visual networks. The RSNs are shown to be composed of brain regions involved in the sensory, motor or higher-order cognitive systems that exhibit correlated intrinsic activity with consistent spatial topographic patterns [32,52,98].

At the mesoscopic level, several network studies have explored age-related patterns in the topological properties of the brain structural and functional networks from regional and global perspectives using graph theoretical metrics of segregation and integration [13,21,42,63,65,84,114]. Overall, previous studies have reported a decline in the connectivity, efficiency and robustness of structural brain networks, suggested to be due to the loss of white matter integrity, neuronal shrinkage, loss of small axon fibers and WM degeneration during aging [13,27,32,114,108]. However, the main brain structural organization has been found to remain relatively intact in healthy aging [114].

Functional network studies have reported more heterogeneous results demonstrating age-related decreases/increases in global and local functional connectivity strength, network segregation, and modularity in healthy aging adults [21–22,43,13,116,11,55,33]. Some discrepancies have been reported between the findings concerning functional connectivity within and between different RSNs in aging studies [32]. Lower age-related connectivity has been consistently found within DMN, frontoparietal control network, dorsal attention network (DAN) and salience networks [6,13,21–22,43]. Reductions in within-network connectivity have also been reported in visual and somatomotor networks associated with aging [13]. In some studies, however, increased age-related within-network connectivity has been found within motor, and subcortical networks, suggested to reflect the compensatory responses to the decreased strength of FC during aging [16,35,99]. In addition, higher between-network connectivity has been found between DMN and DAN in older adults compared to younger individuals [44,91]. Betzel et al. [13] have also found increases in FC among components of dorsal attention, saliency/ventral attention and somatomotor networks. The discrepancy between findings concerning functional connectivity especially at the network level is suggested to be more likely related to physiological confounds or indirect functional interactions relying on synaptic pathways and multiple (parallel) white matter connections [13,62,25,42,45,68,114].

In recent years, neuroscientists' interests have shifted towards exploring the hierarchical integrative architecture of the brain's complex networks. At the macroscopic level, network studies have identified a hierarchical brain structure comprising provincial and connector hubs shown to significantly enhance communication flow within and between multiple communities across the whole-brain network [89,101,54]. In this context, there has been growing interest in identifying densely connected brain hubs forming an embedded network so-called "rich club" (RC) that efficiently links multiple communities across the brain. The RC organization is known to play a critical role in maintaining efficient brain functioning and a high level of resilience, hierarchical ordering, and specialization at the network level [54,21,45]. In healthy adults, the functional and structural rich-club architecture of the brain is shown to display similar topological trajectories [13,32,45]. In previous structural network studies, it is found that the rich club of cortical brain regions consists of medial frontal, medial parietal, insular and subcortical regions [54]. The functional rich club is also found to include brain hubs within medial frontal, medial parietal and occipital regions [21]. Overall, the global integration power of both structural and functional rich-clubs has been found to decline with age [21,114].

A mixture of differences in methodological choices and datasets has led to inconsistency in findings across different studies. The majority of network studies have specifically focused on age-related differences in functional and/or structural connectivity in the same or different cohort of small sample sizes using low-resolution parcellation scales and a limited set of graph measures of network segregation and/or integration [13,114]. The sample size can critically reduce the statistical power especially when one deals with a wide range of ages resulting in sparse data sets across the adult lifespan. The heterogeneity in methodological approaches can make it difficult to compare findings concerning age-related patterns in network topology across different studies. Several factors can affect the reliability of connectivity analysis such as parcellation scales and schemes, type of networks, network normalization and thresholding, type of graph metrics, and preprocessing procedures (smoothing, global signal regression, movement regression) [18,96]. In addition to technical differences, the aging trajectory of the structural and functional rich club interconnecting resting-state networks [54], as well as the brain network vulnerability to perturbations targeting rich club connectivity across the adult lifespan have gained little attention in previous studies of brain connectivity and network topology.

On the basis of these limitations, we performed a comprehensive series of exploratory analyses to investigate age-related trends in the structural and functional connectivity of large-scale brain networks across the adult lifespan from local, global and hierarchical perspectives. At the local and global (mesoscopic) level, age-related differences in the topology of brain structural and functional networks were investigated using graph theoretical metrics of network segregation and integration in a relatively large cohort of healthy aging participants. We also investigated associations between age-related functional and structural connectivity patterns and

cognitive decline. At the network hierarchy level, age-related shifts in the hierarchical RC organization of the functional and structural connectome were explored. At the cross-modal level, we assessed age-related patterns in the RC involvement of sensory-motor and higher-order processing RSNs, subcortical regions and cerebellum. Additionally, we explored the coupling between functional and structural connectivity within RSNs as well as the whole-brain network across the adult lifespan. Finally, we evaluated the age-related vulnerability of both the structural and functional brain networks to damage by selectively removing rich-club nodes and re-assessing the network efficiency.

Materials and methods

Participants and MR data

Neuroimaging data from a total of 619 healthy aging individuals aged 18 to 88 years (mean age = 54.5 ± 18.4 years) from the Cambridge Centre for Ageing and Neuroscience repository (CamCAN, Stage 2, [83,95] were included in this study after excluding participants with poor image quality, excessive head motion or rotation, missing or incomplete data. Ethical approval for the study has been obtained from the Cambridgeshire 2 (now East of England-Cambridge Central Research Ethics Committee), and all participants gave full informed consent.

The structural and functional imaging data were acquired from participants in a single 1-hour session at a single site (MRC-CBSU) using a 3 T MRI scanner (Siemens TIM Trio) with a 32-channel head coil. T1w images were acquired with a 3D Magnetization-Prepared Rapid Acquisition Gradient Echo (MPRAGE) sequence (TR/TE = 2250/2.99 ms; inversion time (TI) = 900 ms; flip angle = 9°; FOV = 256 × 240 × 192 mm^3; voxel size = 1 × 1 × 1 mm^3; and GRAPPA acceleration factor = 2). DWI data were collected with a twice-refocused spin-echo sequence (30 diffusion gradient directions for two b-values: 1000 and 2000 s/mm^2, along with three images acquired using b-value of zero; TR/TE = 9100/104 ms; voxel size = 2 × 2 × 2 mm^3; FOV = 192 × 192 mm^2; number of slices = 66).

For rsfMRI measurements, 261 volumes (lasting 8 min and 40 s) of resting-state functional MR images were acquired from each subject with an echo-planar imaging (EPI) sequence. Each volume included 32 axial slices (acquired in descending order), with a slice thickness of 3.7 mm and inter-slice gap of 20 % (for full brain coverage including cerebellum), TR/TE = 1970/30 ms; flip angle = 78°; FOV = 192 × 192 mm^2; voxel-size = 3 × 3 × 4.44 mm^3). During the resting-state scan, all participants were required to lie still while keeping their eyes closed.

To investigate associations between age-related functional and structural connectivity patterns and cognitive decline, we used three cognitive (visuospatial, language, and memory) scores obtained using Addenbrooke's Cognitive Examination (ACE-R) [69], from all participants grouped into seven age deciles (Table 1).

Processing pipeline

Fig. 1 shows the processing pipeline for multimodal brain network connectivity analysis across the adult lifespan at three levels. The first-level (mesoscopic) network analysis focused on exploring age-related differences in the topology of functional and structural networks consisting of cortical, subcortical and cerebellar regions across the adult lifespan using graph-theoretical approaches from both local and global perspectives. At the network hierarchy level, differences in the hierarchical organization of the functional and structural connectome were explored using the rich-club analysis across different age groups. At the cross-modal level, age-related differences in the involvement of the rich club interconnecting functional modules (RSNs) were investigated. In addition to the main processing steps, the structure–function coupling and the network vulnerability to attack on RC nodes within different functional

Table 1
Clinical and demographic data across age deciles used in this study.

Age (years)	N	Gender (M/F)	Handedness	Education				Memory score	Language score	Visuo-spatial score
				No education	GCSE	A-levels	Higher education			
18–29	67 **(10.8 %)**	27/40	75 ± 50.4	0	3	18	46	24.6 ± 2.1	25.4 ± 0.9	15.6 ± 0.8
30–39	93 **(15 %)**	48/45	79.5 ± 46.7	1	9	12	71	24.7 ± 1.9	25.6 ± 0.8	15.7 ± 0.5
40–49	103 **(16.7 %)**	50/53	75.1 ± 52	2	19	17	65	24.5 ± 1.9	25.4 ± 0.8	15.7 ± 0.6
50–59	91 **(14.7 %)**	49/42	70.1 ± 60.7	4	22	20	45	24.3 ± 2.0	25.2 ± 1.15	15.5 ± 0.8
60–69	101 **(16.4 %)**	47/54	77.3 ± 50.8	13	26	20	42	23.8 ± 2.4	25.2 ± 1.0	15.5 ± 0.7
70–79	104 **(16.8 %)**	54/50	81.7 ± 46.4	23	19	20	42	23.0 ± 3.5	24.7 ± 2.7	15.0 ± 1.9
80–89	60 **(9.6 %)**	33/27	86.8 ± 38.3	18	16	14	12	22.3 ± 3.9	24.8 ± 1.3	15.3 ± 1.0
Total	619	308/311	77.6 ± 50.2	61	114	121	323	24 ± 2.7	25.2 ± 1.5	15.5 ± 1.0

GCSE: General Certificate of secondary Education; A-levels: General Certificate of Education Advance Level; Higher education: College, undergraduate or graduate degree. Handedness measured on a scale from −100 (strong left-handedness) to 100 (strong right-handedness), with 0 indicating ambidexterity.

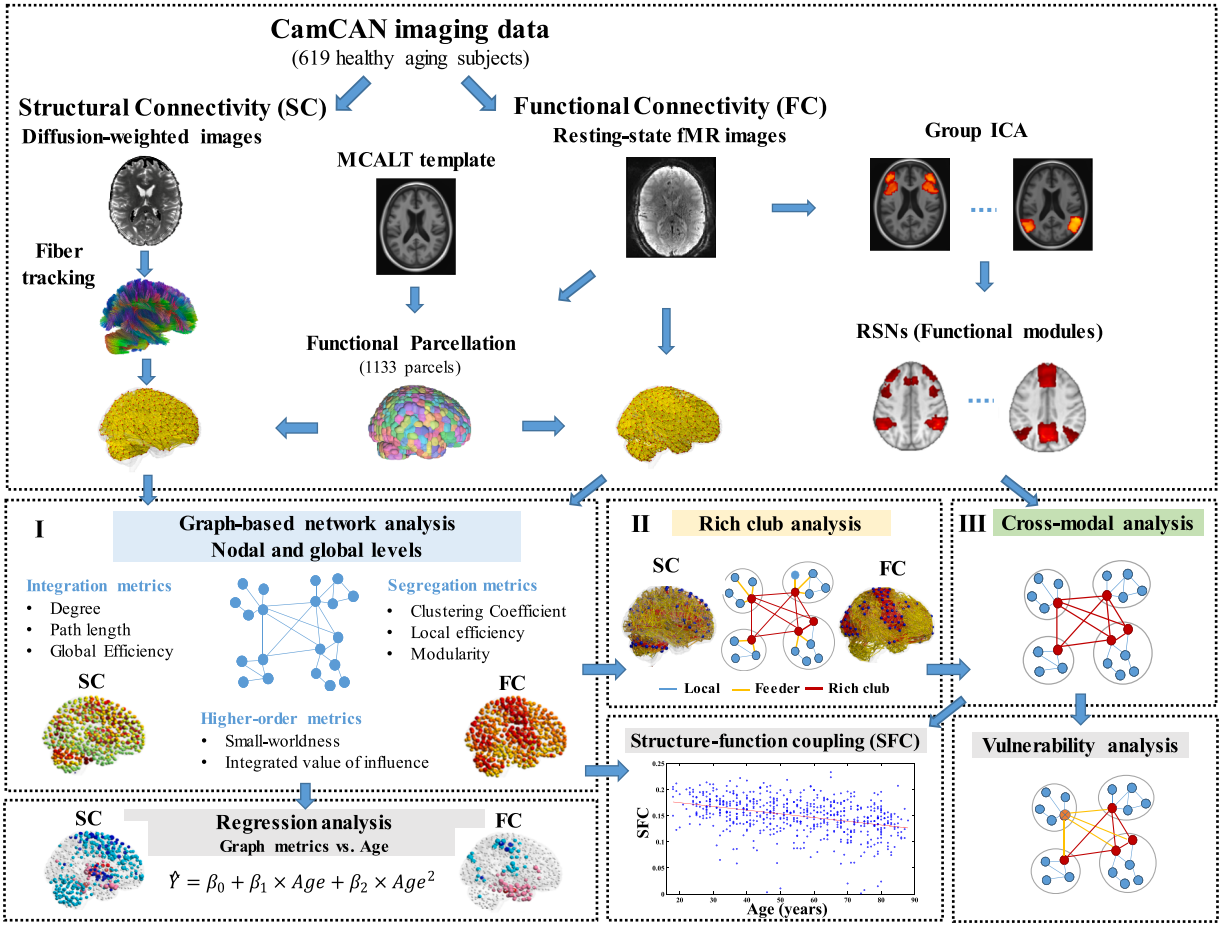

Fig. 1. Processing pipeline for multimodal brain network connectivity analysis across the adult life span at the mesoscopic (I), network hierarchy (II), and cross-modal (III) levels. At each level, associations between structural and functional connectivity patterns as well as structure–function coupling and age were investigated using regression analysis. The vulnerability analysis was used to assess the vulnerability of the structural and functional brain networks to damage to rich-club nodes.

subsystems (RSNs) were evaluated across the adult lifespan. In what follows, the technical details on the procedures illustrated in Fig. 1 and the rationale behind them will be elucidated.

Preprocessing

T1w preprocessing: The T1w images were aligned and normalized to the Mayo Clinic Adult Lifespan Template (MCALT, https://www.nitrc.org/projects/mcalt/) using the affine registration (FSL-FLIRT) [57] and non-linear registration (FSL-FNIRT) tools [40]. Compared to previous network studies on aging that have mostly used MNI templates derived from young healthy subjects, we used the MCALT template constructed from T1-weighted scans of 202 subjects evenly selected from male/female young (age 30–49) and older individuals (age 50–89) to better characterize structural differences across the adult lifespan especially for older adults often displaying enlarged ventricles and sulci and varying degrees of atrophy in gray and white matter [78]. We then used AFNI's 3dSkullStrip to perform skull stripping followed by an automated tissue-type segmentation using FSL-FAST [113] to yield masks of brain compartments including gray matter, white matter and cerebrospinal fluid (CSF).

FMRI preprocessing: AFNI was used to preprocess the rsfMRI data (https://afni.nimh.nih.gov/). The first four image volumes were initially discarded from the resting data of each subject to avoid T1 equilibration effects. Large transient fluctuations were then removed based on the median absolute deviation using AFNI's 3D DESPIKE. Following the slice-timing correction using the middle slice of each volume (AFNI's 3dTshift), a rigid body alignment (AFNI's 3dvolreg) was carried out to estimate movement parameters for each subject using the mean volume. For each subject, frames with excessive head motion (greater than 3.0 mm) and rotation (over 3.0°) were excluded from the subject's time series. Additionally, participants with more than 50 % of frames removed were excluded from the functional connectivity analysis (Table S1), following the approach described by Grayson et al. [45]. On average, less than 0.1 % of frames per subject were excluded from the fMRI data of the remaining subjects. The retained frames exhibited head motion and rotation within the median and interquartile range, as detailed in Table S1. The images were then co-registered with the structural data and spatially normalized into the MCALT space [40], resliced to 3 mm × 3 mm × 3 mm voxels, and smoothed using a Gaussian

kernel with a Full Width at Half Maximum (FWHM) of 6 mm.

In the present study, global signal regression was not applied to remove global artifacts driven by motion, respiration and other noise signals with non-neural origin, given that the global signal regression analysis can discard globally distributed neural information and introduce artificially anti-correlations between certain brain regions, causing increases in specificity and decreases in sensitivity of correlation measures or even reducing the reliability of graph metrics [18,96]. Instead, we regressed out the mean WM and CSF signals as temporal covariates through multiple linear regression analysis [28]. To this end, lower-resolution masks (3 mm isotropic) were generated for WM and CSF from the high-resolution segmented T1w images for each participant to match the rsfMRI data. The mean WM and CSF signals were then computed by averaging signals over all voxels within the WM or CSF masks. Nuisance noises such as linear trends, 12 head-motion parameters, and individual mean WM and CSF signals were then regressed out using multiple linear regression analysis. Finally, the rsfMRI data were temporally band-pass filtered within 0.01 and 0.1 Hz as suggested by [28].

DWI preprocessing: We first used the quality control procedure described by Yeh et al. [111] to examine the integrity and quality of DWI data for each subject. The three-b0 images were then used to estimate the susceptibility field distortion [10] for susceptibility distortion and eddy current correction using the non-parametric approach (FSL EDDY) [4,5].

The preprocessed DW images were then used to fit the diffusion profile in each voxel in the native space by performing the non-parametric generalized q-sampling imaging (GQI) method in DSI-Studio [110]. The deterministic streamline tractography (Euler Tracking algorithm) was then employed to generate 1,000,000 streamlines [60] for each subject by performing random seeding within the entire white matter volume. The quantitative anisotropy (QA) was calculated for the orientation distribution function peak in each voxel. The QA enabled direction-specific thresholding during tractography such that the tracking algorithm terminated if a voxel had a low QA value less than Otsu's threshold of 0.8 [72]. This threshold was used to maximize the variance between background and foreground voxels. The angular threshold and step size were set to 45° and 0.75 mm, respectively [66]. Tracks shorter than 30 mm or longer than 300 mm were then discarded as suggested by Khalilian et al. [60]. Finally, topology-informed pruning [109] was applied in two iterations to remove false connections.

Age-related differences in structural and functional connectivity

To date, most network studies on age-related changes in both structural and functional connectivity across the human lifespan have used anatomical parcellation schemes at coarse to intermediate scales involving less than 400 cortical and subcortical parcels [13,45,84,107,112,114]. For graph-based brain network analysis at the macroscale, the node definition (size and number) and parcellation scheme should ensure functional homogeneity of brain parcels and spatial continuity (necessary conditions required to preserve the interpretability of the connectivity results) all by retaining functional heterogeneity between parcels [37]. While coarse representations can reduce conditionality and variability, resulting in computational and statistical benefits due to dimensionality reduction [86], the discrepancy between connectivity results obtained using coarse parcellations is more likely caused by nodes that combine functionally heterogeneous brain regions into a single entity. Therefore, it is important to use a functional parcellation scheme to delineate functionally homogenous parcels using a high-resolution parcellation scheme required to split small brain regions like the thalamus comprising many functionally heterogeneous sub-nuclei [50] or cerebellum, within which a structural parcellation based on anatomical landmarks is less efficient [24]. Moreover, a high spatial resolution is shown to be more representative of the brain and essential to ensure the reproducibility and stability of network topological properties [38,54,60,114].

On the basis of these criteria, we used the spatially-constrained normalized-cut spectral clustering algorithm introduced by Craddock et al. [29] to derive a whole-brain functional parcellation comprising 1133 parcels within cortical and subcortical regions, deep gray matter and cerebellum across the entire aging population in the MCALT template space based on the region homogeneity and spatial contiguity conditions. In this method, clustering is first performed based on correlation values between voxels' time courses to generate parcels at the single-subject level. Then, a group-wise clustering is carried out by clustering the average of the individual connectivity maps. We used the same parcellation for both structural and functional connectivity analyses.

For structural connectivity analysis, an $N \times N$ weighted connectivity matrix was constructed for each subject, in which N was the total number of nodes and edges were the number of streamlines connecting pairs of nodes. To discard spurious connections that were potentially influenced by noise, the edges that included less than 10 streamlines were set to zero [60]. For group comparison, a subject-wise normalization was performed by multiplying each edge's weight by its QA value and then normalizing it to the total number of streamlines in the corresponding weighted matrix [13]. For group analysis, a group-weighted structural connectivity matrix was computed for each age decile by averaging the connections that were present in at least 75 % of the subjects in the group [54].

For functional connectivity analysis, a weighted functional connectivity matrix was calculated for each subject, in which connection strengths were Pearson's correlation coefficients between the average time series of all node pairs. Group-average functional connectivity networks were then estimated across subjects in different age deciles. Due to the large number of exploratory analyses that required extensive computational demands in this study, we used a single optimal proportional threshold estimated using the method introduced by Bassett et al. [8] across different age deciles. In this method, a cost-efficiency curve was first estimated over a wide range of thresholds (0.05–0.5) for each age decile by generating sparse and low-cost adjacency matrices (0.05) to densely connected or high-cost graphs (0.5). We found an optimal threshold of 0.2 by maximizing global cost-efficiency across all age ranges. This threshold was subsequently employed to binarize the group functional connectivity matrices.

First-level network analysis. The first-level network analysis focused on exploring age-related differences in the topology of functional and structural networks across the adult lifespan from both local and global perspectives.

To assess differences in the global topological properties of the whole-brain structural and functional brain organization across different age ranges, we computed global metrics including mean strength/degree (K), global efficiency (E_g), clustering coefficient (C_c) and small-worldness (SW) for each participant. We further computed nodal graph measures including strength/degree, local efficiency (E_L), and clustering coefficient [39] to examine age-related differences in the topological properties of individual regions. In this study, global and nodal metrics were computed for weighted structural graphs and binarized functional graphs (see Section 2.2.2 for more details).

Hierarchy-level network analysis. At the network hierarchy level, age-related differences in the hierarchical (rich club) organization of the functional and structural connectome were investigated using the rich-club analysis described in Heuvel and Sporns [54] across different age deciles. In this approach, a rich club is determined as a set of nodes with an interconnectivity level exceeding the expected level of connectivity in random networks. For each group structural and functional network, a rich club coefficient $\Phi(k)$ was computed for each degree k varying from 1 to the maximum degree in the network as follows:

$$\phi(k) = \frac{2.E_{\geq k}}{N_{\geq k}(N_{\geq k} - 1)} \tag{1}$$

where, after removing all N nodes with a degree less than k, $E_{>k}$ and $N_{\geq k}$ represented the number of connections between the remaining nodes in the network and the total number of possible connections between the remaining nodes if there were fully connected, respectively. For each group network, a normalized rich-club coefficient $\Phi_{norm}(k)$ was computed with respect to $\Phi_{random}(k)$, as the average rich-club coefficient over m (herein 10,000) random networks of equal size with similar connectivity distribution, generated by randomizing the connections of the network while keeping the degree distribution of the matrix intact [54]. The rich club range was then defined over k levels whose $\Phi_{norm}(k)$ were greater than one. In general, the choice of the k level is arbitrary and study-dependent [60]. To compare the spatial rich-club distribution across different age deciles, we selected a k level for each age decile such that the top 30 % of high-degree nodes in each group network were in the rich club. This k level was selected based on the trade-off between spatial homogeneity and inter-hemispheric symmetry. Moreover, lower or higher thresholds resulted in dense or sparse RC maps including RC nodes that exhibited low or very high rich-clubness, respectively.

To better investigate the hierarchical structure of the brain networks, the group network edges were further into rich-club, feeder and local connections, defined as connections linking members of the rich club nodes, rich club to non-rich club nodes, and non-rich club nodes, respectively [102]. For each group connectivity matrix, an average physical length (in mm) was also computed for each edge by averaging the physical lengths of the streamlines over the subjects in each age group. The physical length was used as a measure to further investigate the spatial distribution of short-range (SR) and long-range (LR) rich club, feeder, and local connections based on their average physical lengths shorter and longer than the median of all physical lengths (herein 70 mm for structural networks and 50 mm for functional networks), respectively [114]. For the group functional networks, the physical length for each edge was defined as the distance between the centroids of the parcels connected by the edge.

In addition to rich-club nodes, as a unique feature of our study, we used the Integrated Value of Influence (IVI) to identify the most influential brain hubs also called “spreaders” shown to have higher impacts on the flow of information across the whole-brain network [61]. The IVI is an integrative measure of segregation and integration of information, computed based on the local (i.e. degree centrality, ClusterRank, neighborhood connectivity and local H-index) and global (i.e. betweenness centrality and collective influence) measures [82]. Numerical calculations were performed using the computational resources of the MATRICS platform at University of Picardy Jules Verne, Amiens, France.

Cross-modal structural–functional analysis. To test the hypothesis that aging could significantly affect the rich-club involvement of different functional subsystems (RSNs), we performed a cross-modal structural–functional analysis, in which RSNs were first identified by decomposing the preprocessed rsfMRI data using the group spatial independent component analysis (gICA, GIFT toolbox) [20] across. In this method, the time point data from each subject were first reduced to 40 directions of maximal variability using the principal component analysis (PCA). The group PCA-reduced matrix was then decomposed by the infomax algorithm into 60 principal components (PCs) along directions of maximal group variability. A voxelwise variance normalization was performed for the decomposition of subcortical and cortical components. The ICA algorithm was repeated 20 times and the resulting independent components (ICs) were clustered by the ICASSO software to obtain a set of 60 aggregated spatial maps (SM) and their time courses (TCs). The subject-specific SMs (and TCs) were computed using the back reconstruction approach [20], processed using voxelwise one-sample t-tests ($p < 0.01$) across all subjects, and then thresholded to obtain regions of peak activation for each component [3]. We empirically determined the optimal number of PCs and ICs employed for the decomposition of the rsfMRI data, guided by the spatial and temporal characteristics of the components required to represent meaningful and spatially coherent patterns consistent with established resting-state networks. This selection process was performed by the examination of component consistency across different age groups through visual inspection. We then performed the group ICA on resting-state fMRI data separately for each age group to account for age-related heterogeneity in functional brain connectivity. It allowed for a more detailed and accurate characterization of the unique functional connectivity patterns within different age groups, contributing to a better understanding of the dynamic nature of the human brain throughout adulthood.

Among the 60 ICs, an average (across age groups) of 40 (± 3) components exhibited peak activations in grey matter and were selected and grouped based on their spatial coordinates and prior knowledge from other fMRI studies [3,31] into nine resting-state networks (RSNs) including visual network (VIS), default mode network (DMN), cerebellar network (CBN), cognitive control-

attention network (CAN), subcortical network (SCN), sensory-motor network (SMN), language-auditory network (LAN), temporal network (TMN) and limbic network (LMN). The definition of the RSNs was primarily derived from prior rsfMRI studies [3,31]. In summary, the sensory and motor networks (SMN, VIS, and LAN) comprised brain regions engaged in processing visual, auditory, and other sensory information, as well as coordinating motor responses. Specifically, LAN also encompassed regions associated with language processing. The DMN and CAN comprised regions involved in higher-order information processing, cognitive control, and attentional processes. The limbic network (LMN) included brain regions involved in the regulation of emotional responses. For the remaining RSNs (CBN, SCN, and TMN), given their extensive involvement in various cognitive, sensory, and motor control functions, we grouped ICs whose activation maps overlapped with brain regions located in the respective networks.

The components showing peak activations in white matter or high spatial overlap with vascular, ventricular, motion and susceptibility artifacts were discarded from further analysis [2]. For the cross-modal structural–functional analysis, each node (parcel) was assigned to a single RSN using the "winner-take-all" strategy [54], such that the minimum overlap between the parcel and the RSN was more than 10 %.

At the macroscopic level, a hierarchical brain structure is shown to comprise provincial and connector hubs as key players in enhancing communication flow within and between functional modules across the whole-brain network [54]. To identify these hubs, we used the approach employed by Heuvel and Sporns [54]. In this method, nodes were classified based on their within-module degree z-score (z_s) and participation coefficient (p_c) using the functional modules [46] into peripheral nodes (low z_s and low p_c), non-hub connector nodes (low z_s and high p_c), provincial hubs (high z_s and low p_c), and connector hubs (high z_s and high p_c). In our study for the group structural networks, the thresholds for "high z_s" ($z_s > 1.25$) and "high p_c" ($p_c > 0.3$) were determined based on the guidelines suggested in the literature [46,89]. For the group functional networks, the estimated thresholds were set to ($z_s > 1$) for "high z_s" and ($p_c > 0.7$) for "high p_c".

Based on this classification, we computed the proportion of RC, connector and provincial hubs for each RSN and that of rich-club, feeder and local inter-RSN (between-RSN) and intra-RSN (within-RSN) edges for each age decile [54].

Finally, high-ranked rich-club AAL regions in the structural and functional brain networks were identified across different age deciles using weighted rich-club scores computed for all AAL regions in the MCALT-ADIR122. For this purpose, a normalized rich club score was first calculated for each AAL region [100] based on its overlap with all rich club regions [38] for each age group. The average rich-club score was then computed over the seven age deciles. The cross-age high-ranked AAL rich-club regions were identified as those exhibiting an average rich club score higher than 1 across all the seven age deciles.

Age-related differences in network topological properties

To investigate age-related differences in the topological properties of the brain networks across the adult lifespan, a regression analysis was performed at the nodal level with age and age^2 as predictors:

$$\widehat{Y} = \beta_0 + \beta_1 \times Age + \beta_2 \times Age^2 \tag{2}$$

where $\widehat{Y}$ was a vector of estimations of y, i.e. values of nodal graph measures including degree, clustering coefficient, local efficiency, IVI and average physical length computed for each subject, β_1 and β_2 were regression coefficients for the linear and quadratic models, and β_0 was the intercept term. One-sample t-tests were performed to investigate whether the models exhibited an age effect with a significance level of $p < 0.01$ (FDR-corrected). The regression analysis was also performed at the network level to examine the relationship between SW, global efficiency or mean clustering coefficient and age as well as each of the three cognitive scores (visuospatial, language, and memory).

Age-related differences in structure–function coupling

The coupling between the functional and structural connectomic strengths has been reported to be heterogeneous across the brain, showing a declining trend with age [14,70,32,94]. To investigate age-related differences in the coupling between the structural and functional connectome, we first computed Pearson's correlation coefficients between the connection strengths (constrained by non-zero edges) and nodal measures (degree, clustering coefficient and local efficiency) of the structural and functional connectivity matrices for each participant. The correlation analysis was then performed to assess linear associations between SFC and age within each RSN and at the whole-brain network with $p < 0.05$.

Age-related differences in network vulnerability to damage to RC nodes

It is largely believed that any damage to RC regions can cause widespread disruption across large-scale brain networks with a significant impact on cognition and behavior [1,59]. However, the extent to which the whole-brain structural and functional networks are vulnerable to the loss of RC nodes within different RSNs is largely unknown at different age deciles.

To investigate the network vulnerability to damage to rich club nodes in each RSN, each RC node i was removed from the group functional and structural networks and the network vulnerability index was calculated as:

$$V_i = \frac{E_N - E_i}{E_N} \tag{3}$$

where E_N and E_i were the global efficiency of the network before and after the attack. The average vulnerability index was then computed over all RC nodes within each RSN. Differences in network vulnerability across different aging groups were assessed using non-parametric Kruskal-Wallis tests with $p < 0.01$.

Results

Age-related differences in topological properties

We conducted nodal and global-level network analyses to investigate disparities in both brain structural and functional connectivity among adults spanning the entire lifespan. This encompassed examinations of localized brain regions as well as an exploration of the overall network architecture.

Nodal metrics

The nodal-level graph analysis of structural brain networks unveiled distinct age-related patterns of connectivity as illustrated in Fig. 2 and Table 2. At all age ranges, the nodes exhibiting higher strength (K), clustering coefficients (C_C), and IVI were associated with longer mean fiber lengths (Fig. S1), predominantly localized within the bilateral frontal regions (including the superior and middle frontal gyri), central and parietal regions, the cerebellum, and subcortical regions, along the anterior-posterior medial axis of the brain. In structural networks, many nodes in the medial frontocentral regions, and the cerebellum displayed either linearly declining trends (r: -0.24 ± 0.1, $p < 0.01$, FDR corrected) or followed inverted-U shaped trajectories for K, C_C, and/or IVI with increasing age, all associated (r: 0.12 ± 0.01) with declines in cognitive scores, especially the memory score. In contrast, several structural nodes within subcortical regions, specifically the thalamus, pons, and putamen, as well as temporal and parieto-occipital regions, exhibited increasing linear (r: 0.15 ± 0.05) or inverted U-shaped trends in strength, C_C, or IVI with age.

The analysis of functional networks revealed distinctive age-related patterns in the distribution of network properties across various brain regions. Specifically, irrespective of age, functional nodes with higher values of K, CC, along with increased IVI, were primarily located in the prefrontal, centrotemporal, and occipital, as well as the cerebellum, predominantly associated with longer physical distances, as shown in Fig. S1. Within the centrotemporal and occipital regions, as well as the cerebellum, a few sparsely distributed functional nodes exhibited a significant linear decline in degree with age (r: -0.13 ± 0.02, $p < 0.01$). In contrast, the temporal regions displayed an inverse trend with a positive correlation (r: 0.14 ± 0.02). Compared to degree centrality, age-related differences in C_C were more pronounced in numerous functional nodes within the bilateral frontal and temporo-parietal regions, as well as the cerebellum, demonstrating increases in C_C (r: 0.14 ± 0.028) in older individuals (Figs. 2 and S1).

Among the most influential functional nodes, only those in the temporal regions exhibited a significant increase in IVI with age (see Fig. 2). Moreover, a significant association (r: 0.12 ± 0.01) was observed for most of the functional nodes between age-related trends in nodal metrics and declines in at least one of the cognitive scores. In the case of the functional networks, no distinct age-related spatial patterns were observed in the mean physical distance.

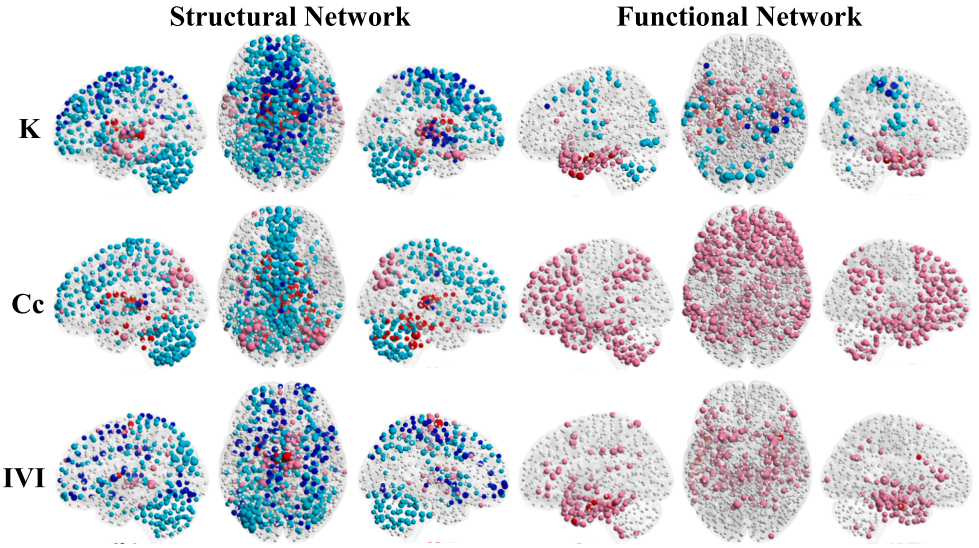

Fig. 2. Age-related differences in nodal metrics (K: strength/degree, C_C: clustering coefficient, IVI: Integrated Value of Influence) in association with cognitive scores (visuospatial, language, and memory) for structural and functional brain networks. The nodal color indicates positive (Pink: linear, Red: quadratic) or negative associations (Cyan: linear, Blue: quadratic) found using regression analysis ($p < 0.01$, FDR-corrected) between nodal metrics and age. Node size represents linear associations between nodal metrics and cognitive scores, categorized in three sizes, small (correlation with only one score), medium (correlation with two scores), and large (correlation with all three scores). (For interpretation of the references to color in this figure legend, the reader is referred to the web version of this article.)

Table 2
Global and local graph measures (median ± standard error) of the structural (SN) and functional (FN) brain networks for each age decile.

			18–29 (yrs)	30–39 (yrs)	40–49 (yrs)	50–59 (yrs)	60–69 (yrs)	70–79 (yrs)	80–89 (yrs)
Global measures	**Small-worldness**	**SN**	6.72 ± 0.74	6.65 ± 0.70	6.62 ± 0.75	6.56 ± 0.72	**6.44 ± 0.77**	**6.40 ± 0.93**	**6.26 ± 0.95**
		FN	1.78 ± 0.13	1.78 ± 0.13	1.78 ± 0.13	1.80 ± 0.14	1.79 ± 0.13	**1.83 ± 0.13**	**1.84 ± 0.14**
	Global efficiency	**SN**	0.42 ± 0.01	0.42 ± 0.01	0.43 ± 0.01	0.42 ± 0.01	0.42 ± 0.02	**0.40 ± 0.03**	**0.39 ± 0.02**
		FN	0.55 ± 0.01	0.55 ± 0.02	0.54 ± 0.03	0.54 ± 0.03	0.54 ± 0.03	**0.53 ± 0.04**	**0.53 ± 0.04**
	Clustering coefficient	**SN**	$3.2e^{-3}$ ± $5.8e^{-4}$	$3.1e^{-3}$ ± $5.2e^{-4}$	**$3e^{-3}$ ± $5.2e^{-4}$**	**$2.9e^{-3}$ ± $5.2e^{-4}$**	**$2.9e^{-3}$ ± $5.4e^{-4}$**	**$2.7e^{-3}$ ± $4.7e^{-4}$**	**$2.8e^{-3}$ ± $5.9e^{-4}$**
		FN	0.50 ± 0.04	0.51 ± 0.05	0.52 ± 0.05	0.52 ± 0.05	0.51 ± 0.05	**0.53 ± 0.06**	**0.53 ± 0.06**
Nodal measures	**Strength**	**SN**	0.75 ± 0.13	0.74 ± 0.14	0.73 ± 0.14	**0.69 ± 0.14**	**0.70 ± 0.14**	**0.61 ± 0.12**	**0.61 ± 0.14**
	Degree	**FN**	211.3 ± 15.5	209.5 ± 18.4	**204.2 ± 17.1**	**205.4 ± 17.6**	**208.3 ± 17.1**	**205.3 ± 19.1**	**203.4 ± 19.9**
	Local efficiency	**SN**	$4.6e^{-3}$ ± $8.1e^{-4}$	$4.4e^{-3}$ ± $7.4e^{-4}$	**$4.3e^{-3}$ ± $7.4e^{-4}$**	**$4.1e^{-3}$ ± $7.4e^{-4}$**	**$4.2e^{-3}$ ± $7.8e^{-4}$**	**$3.8e^{-3}$ ± $6.7e^{-4}$**	**$3.9e^{-3}$ ± $8.5e^{-4}$**
		FN	0.75 ± 0.02	0.75 ± 0.02	0.75 ± 0.02	0.75 ± 0.02	0.75 ± 0.02	0.76 ± 0.02	0.76 ± 0.03
	Clustering coefficient	**SN**	$5.1e^{-3}$ ± $7.5e^{-4}$	**$4.9e^{-3}$ ± $7.7e^{-4}$**	**$4.6e^{-3}$ ± $7.7e^{-4}$**	**$4.6e^{-3}$ ± $7.1e^{-4}$**	**$4.7e^{-3}$ ± $8.5e^{-4}$**	**$4.3e^{-3}$ ± $6.5e^{-4}$**	**$4.2e^{-3}$ ± $8.9e^{-4}$**
		FN	0.50 ± 0.04	0.51 ± 0.05	0.52 ± 0.05	0.52 ± 0.05	0.51 ± 0.05	**0.54 ± 0.06**	**0.54 ± 0.06**
	Physical length	**SN**	12.65 ± 2.33	12.82 ± 2.08	13.12 ± 2.26	12.72 ± 2.50	12.59 ± 2.70	11.98 ± 3.17	**11.41 ± 2.47**
		FN	74.44 ± 2.00	74.50 ± 2.22	74.72 ± 2.19	75.16 ± 2.73	75.42 ± 2.40	75.43 ± 3.58	74.64 ± 2.71

Bold values indicate significant group differences ($p < 0.05$, FDR-corrected) between each age decile and the first age decile (18–29 years).

Global metrics

The global-level graph analysis revealed a small-world topology in both the structural and functional brain networks, regardless of age (Table 2). However, structural brain networks exhibited a declining trend in SW, C_C, and E_g as age increased, as shown in Fig. 3. Specifically, SW and C_C showed linear decreases with age, while global efficiency followed an inverted U-shaped trajectory of decline. In contrast, functional networks showed linear increases in SW and C_C with age, while E_g exhibited an inverse pattern. Overall, the correlation analysis revealed negative associations between cognitive scores ($r_{visuospatial} = -0.17$, $r_{language} = -0.16$ and $r_{memory} = -0.27$ with $p < 0.0001$) and age (Fig. S3).

Rich club organization

We further performed the rich-club analysis to explore differences in the hierarchical organization of the functional and structural connectome between different age deciles. Our results revealed a rich-club organization in both the structural and functional brain networks in each age group, characterized by $\varphi_{norm}(k) > 1$ ($p < 0.005$, 10,000 permutations), with a range of k values falling within [6–114] for the structural networks and [54–117] for the functional networks. The graphical representations of the top 30 % of high-degree rich-club nodes (depicted in blue), as well as rich-club nodes (red), feeder connections (orange), and local connections (yellow),

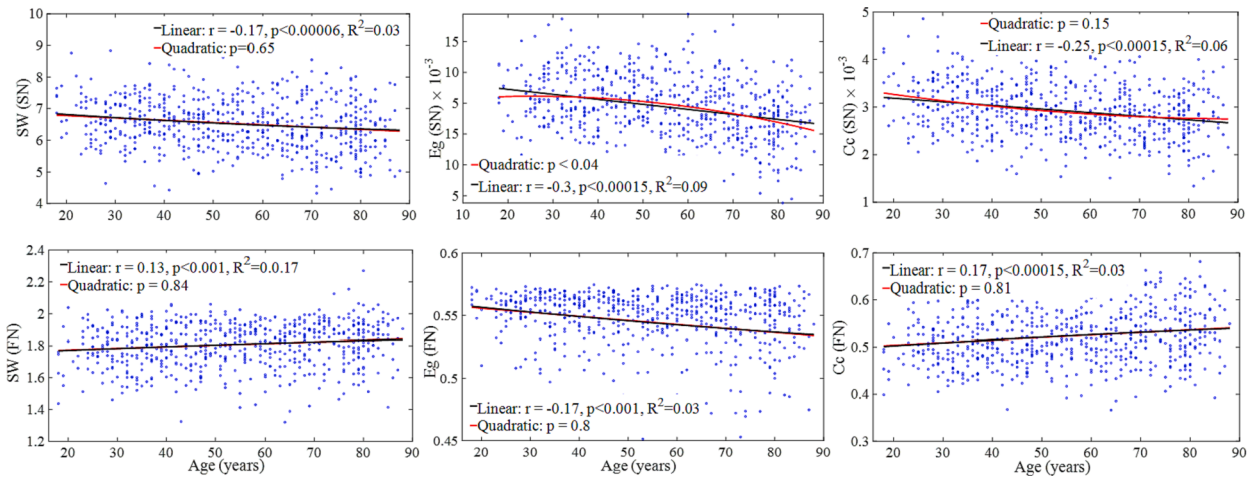

Fig. 3. Results of regression (linear and quadratic) and correlation analyses. The figure depicts correlations between network metrics (SW: small-worldness, E_g: global efficiency, C_C: clustering coefficient) and age for structural (SN) and functional (FN) networks.

are presented in Fig. S4 for each age decile.

Structural rich-club nodes were predominantly distributed along the anterior-posterior axis of the brain, encompassing fronto-central, occipital, subcortical regions, and the cerebellum across all age deciles. In older age ranges, a notable reduction in the number of structural rich-club nodes was observed in the cerebellum.

In younger age ranges, functional rich-club nodes were primarily located in the frontal, centrotemporal, parietal, and occipital regions, as well as the cerebellum. With increasing age, a significant reduction in the number of functional rich-club nodes was mainly observed in the frontal and parietal regions.

In both the structural and functional networks, rich-club and feeder connections extended between brain regions along the anterior-posterior medial axis of the brain throughout all age ranges. It is noteworthy that the majority of local connections were cortico-cortical.

Cross-modal structural–functional analysis

The cross-modal structural–functional analysis yielded findings that support the notion of the rich club acting as a structural backbone connecting functional brain communities (RSNs) across all age groups. However, significant age-related differences in the contributions of the rich club to RSNs were observed, particularly in individuals aged over 70 compared to younger age groups.

Age-related differences in rich-club involvement: Fig. 4 illustrates the rich-club involvement in different RSNs (Fig. S5 and Table S2) for both the structural and functional networks. Within the structural networks, TMN displayed the lowest involvement (2.4 ± 0.6 %) in the structural rich club, while the SCN exhibited the highest involvement (18.2 ± 1.1 %) across all age ranges. CAN (17.1 ± 0.4 %), DMN (14.9 ± 1.1 %), SMN (13.4 ± 0.7 %) and CBN (13 ± 3.4 %) also demonstrated relatively high rich-club involvement. The rich-club involvement of CBN and DMN showed a decreasing trend with age, while SMN, LAN, and SCN exhibited an opposite trend. Other networks displayed only slight age-related differences in rich-club involvement across different age deciles.

In the functional networks, LMN had the lowest contribution (2.9 ± 1.5 %) to the functional rich club, whereas SMN exhibited the highest involvement (24.3 ± 6.2 %). LAN, CAN, VIS, CBN and DMN also showed substantial participation in the functional rich club. Overall, rich-club involvement decreased with age in SMN, DMN, and VIS, and increased in TMN. No specific age-related rich-club pattern was observed for the other RSNs.

More than half of the structural nodes in SCN (62.6 ± 3.9 %) exhibited a high degree of rich-clubness across all age groups (Fig. S6), with even increased proportions in the last two age deciles. Approximately one-third of the nodes in DMN (45.2 ± 3.4 %), CBN (32.3 ± 8.3 %), and SMN (36.1 ± 2.1 %) were identified as part of the rich club. However, a significant reduction in the number of rich-club nodes was observed for DMN and CBN in individuals aged over 70 years. For CAN and VIS, around one-fourth of the nodes exhibited rich-club characteristics and remained relatively stable across different age ranges. Decreased proportions were observed in LMN (12.6 ± 3.9 %) and TMN (4.9 ± 1.3 %). Interestingly, the proportion of rich-club nodes in SMN and LMN increased with age.

In the functional networks, a significant proportion (82.7 ± 21.4 %) of nodes in SMN were part of the rich club across all age ranges, with the highest proportion observed in the middle-age groups. Almost half of the nodes in VIS (50.3 ± 9.7 %) and LAN (42.1 ± 4.7 %) belonged to the rich club. In the remaining RSNs, less than one-third of the nodes were associated with the rich club. In CAN, LAN, SCN, TMN, and LMN, the proportion of rich-club nodes increased in older individuals, while the other RSNs exhibited an inverse trend.

Age-related differences concerning most influential nodes: Characterized by IVI, the most influential nodes within the structural networks were primarily located within SCN and CBN (see Table S3). With the exception of SCN, the mean nodal IVI of RC nodes in the other RSNs showed a significant decrease with age, particularly in the last two age groups. In the functional networks, the rich club nodes in CBN and SMN exhibited significantly increased IVI values. The age-related changes in IVI followed an inverted U-

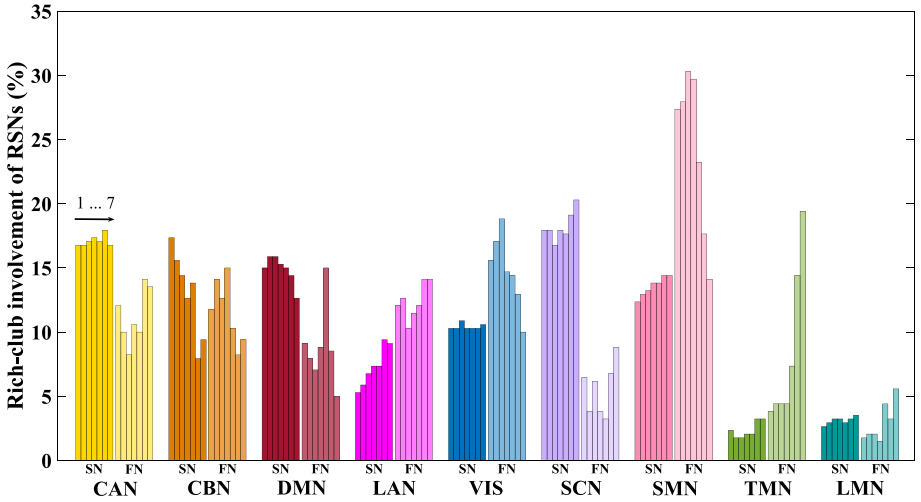

Fig. 4. Overlap between the top 30% of rich-club nodes and RSNs for age deciles 1–7. SN: structural networks, FN: functional networks.

shaped pattern, peaking between the ages of 40 and 60 years.

Age-related differences in proportions of intra-RSN vs inter-RSN connections: In the structural networks, 43 % (±2%) of inter-RSN connections were long-range RC connections, while 34 % (±3%) were feeders. These proportions exhibited increasing and decreasing trends with age, respectively (see Fig. 5). Irrespective of connection type, the proportion of short-range connections increased in older subjects. A similar pattern was observed for intra-RSN connections, albeit with decreased proportions for long-range RC connections (30 % ± 2 %) and feeders (27 % ± 2 %). Across all age ranges, the majority of intra- and inter-RSN connections for DMN, SCN, and LMN were long-range, exhibiting a decreasing trend with age. Conversely, nearly one-third of intra and inter-RSN connections were short-range for other RSNs, following an increasing trend with age. In the functional networks, 22.6 % (±3%) of inter-RSN connections were long-range RC connections, while 34.8 % (±2%) were feeders across all age groups. Notably, the proportion of short-range connections contributing significantly to intra-RSN interactions increased in older individuals. In comparison to the structural networks, older participants exhibited significant increases in the proportion of long-range inter-RSN RC connections in almost all functional networks, except for SCN and CAN, which displayed an inverse trend.

Age-related differences in proportions of RC connector and provincial hubs: A substantial percentage (92.3 ± 2.4 %) of connector hubs were identified as rich club hubs across different age groups in the structural networks (Fig. S7). Among the RSNs, CAN and TMN exhibited the highest (17.4 ± 1.3 %) and lowest (3.8 ± 1.8 %) proportion of RC connector hubs, respectively. The proportion of structural RC connector hubs in VIS, TMN, CBN, LAN, and LMN showed a slight increase with age. Conversely, SCN displayed a significant reduction in the number of RC connector hubs in individuals older than 70 years. When compared to connector hubs, only CAN, CBN, SMN, LAN, and SCN contained nodes with characteristics of provincial hubs. On average, 49.8 % (±8.5 %) of the provincial hubs in CAN were part of the rich club across different age deciles. The proportion of RC provincial hubs increased significantly in SMN and LAN for the last two age groups, whereas a reverse trend was observed for CBN with a cutoff at the age of 70 years. In the functional networks, the proportion of RC connector hubs exhibited an increasing trend with age for TMN and CAN. However, in DMN and CBN, the proportion of RC connector hubs decreased with age. Unlike the structural networks, there was no overlap found between provincial hubs and rich club nodes in the functional networks.

Cross-age high-rank RC regions: Fig. 6 illustrates rich-club regions exhibiting relatively high rich-club scores among the top 30 % of high-degree nodes across different age groups. In the structural networks, the high rank rich-club regions were identified in deep structures (pons, putamen, thalamus, caudate), the cerebellum, frontal regions (superior and middle frontal), precentral gyri (PreCG), insula, anterior cingulate gyrus, median cingulate and paracingulate gyri (DCG), supplementary motor area (SMA), paracentral lobule (PCL), superior temporal gyrus (STG), parietal regions (precuneus), and occipital regions (superior occipital gyrus, SOG). Notably, the superior frontal gyri (SFG) and cerebellum exhibited decreasing rich-club scores with age, while the rich-club scores of PreCG, thalamus, STG, and SOG increased with age. The remaining regions showed subtle differences in rich-club characteristics across different age ranges. In the functional networks, the rich-club regions with higher RC scores were primarily located within the precentral and postcentral gyri, cerebellum, insula, frontal regions, middle and superior temporal gyri, and occipital regions. Most of these regions displayed high rich-club scores that decreased with age, especially in individuals older than 60 years. Interestingly, the rich-club score of the bilateral middle temporal gyri (MTG) significantly increased in older subjects.

Age-related differences in structure–function coupling (SFC)

SFC between connection strengths: Our results indicated positive couplings ($r < 0.21$) between the structural and functional connection strengths, linearly declining ($r = -0.38$) with age (Fig. S8) at the whole-brain network. Our results further revealed a significant reduction in SFC with age for.

CBN ($r = -0.45$), CAN ($r = -0.29$), SMN ($r = -0.25$) and SCN ($r = -0.21$). We also found a decrease in SFC with age for DMN and TMN, however, with a lower declining rate ($r = -0.17$) in comparison with sensorimotor cortices. Among all RSNs, no age-related differences in SFC between connection strengths were observed in auditory, language, visual and limbic systems.

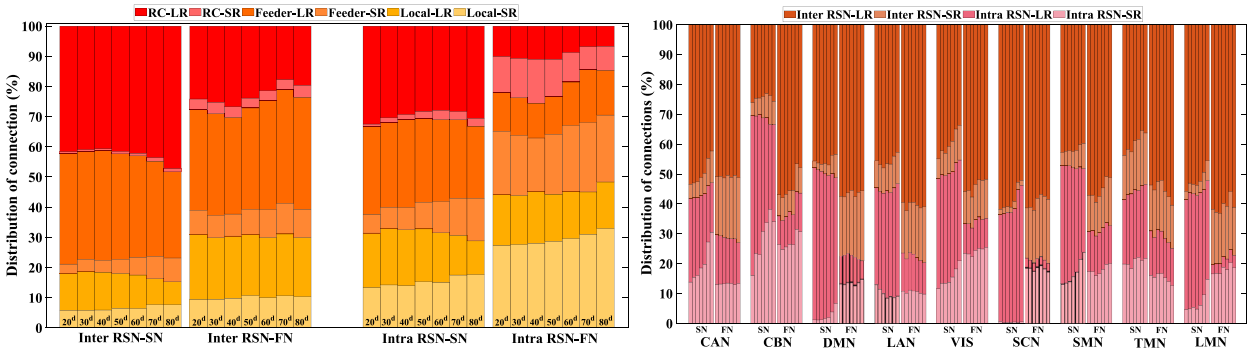

Fig. 5. Proportion of intra-RSN and inter-RSN rich club (RC), feeder, and local connections categorized into short-range (SR) and long-range (LR, and proportion of intra-RSN and inter-RSN short-range and long-range connections for each age decile. SN: structural networks, FN: functional networks.

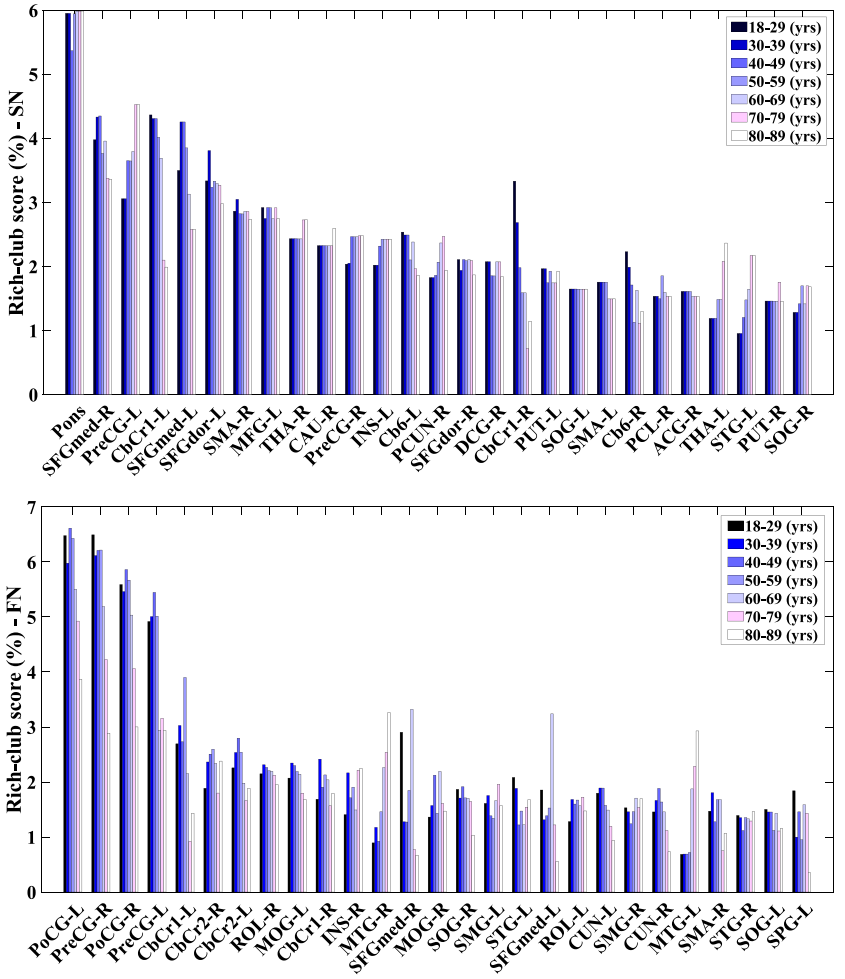

Fig. 6. High-rank rich club AAL regions for each age decile. SN: structural networks, FN: functional networks.

SFC between nodal measures: At the network level, we observed a mild declining trend ($r \approx -0.1$) in the coupling between nodal degree and efficiency for both structural and functional networks with increasing age. Likewise, the coupling between the structural and functional degree decreased.

($r < -0.17$) with age for nodes within the LMN and CBN. Interestingly, within the LAN, the strength of the coupling between nodal degree and efficiency increased ($r < 0.23$) with age.

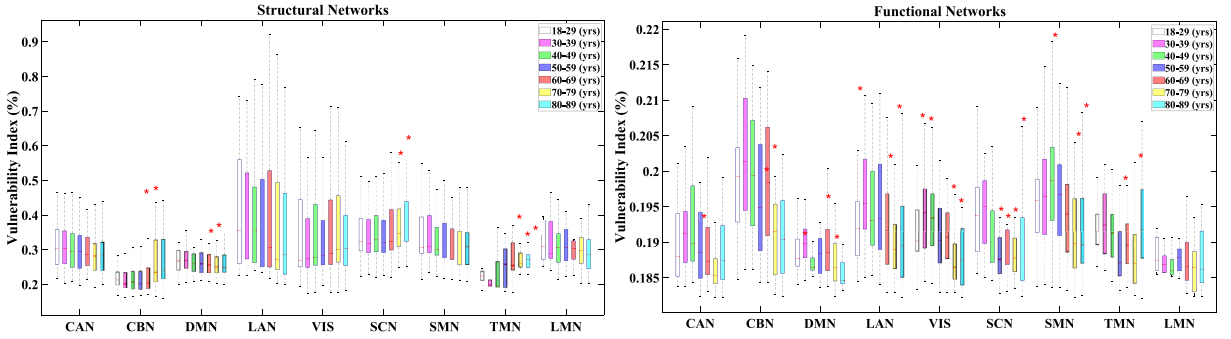

Fig. 7. Quantile box plots of the vulnerability index for structural and functional networks. The network vulnerability was assessed to damage to RC nodes within each RSN for each age decile.

Age-related differences in network vulnerability to targeted attacks on RC nodes

Fig. 7 illustrates the network vulnerability to damage to RC nodes within each RSN for both the structural and functional brain networks at each age decile. The structural networks, regardless of age, exhibited high vulnerability to attacks on RC nodes within LAN, VIS, and SCN, with comparatively lower vulnerability in CBN and TMN. Notably, the overall network vulnerability to attacks on RC nodes significantly increased with age in CBN, SCN, and TMN ($p < 0.01$). In contrast, an inverse trend was observed for DMN. The age-related trend in network vulnerability for the remaining RSNs showed no specific pattern.

For the functional networks, greater vulnerability was observed when RC nodes within CBN, LAN, and SMN were targeted, while the networks were more resilient to attacks on RC nodes in DMN and LMN. In older age groups, the vulnerability of the functional network to the loss of RC nodes decreased across all RSNs, particularly within CBN, DMN, SCN, and TMN. For VIS and SMN, the functional network vulnerability followed an inverted U-shaped trajectory with age.

Summary of age-related differences in connectivity patterns across multilevel analyses

Table 3 summarizes the key findings regarding age-related differences in connectivity patterns at various levels of connectivity analyses.

Table 3
Summary of age-related differences in connectivity patterns at nodal, global, hierarchical, and cross-modal levels.

Nodal level	SN	Regardless of age	Nodes with higher K/C_C/IVI were located along the anterior-posterior medial axis of the brain within o Frontal, central and parietal regions o Subcortical regions o Cerebellum
		Older vs. Younger individuals	• Decrease in K/C_C/IVI in medial frontocentral regions and cerebellum • Increase in K/C_C/IVI in subcortical, temporal and parietal regions
	FN	Regardless of age	Nodes with higher K/C_C/IVI were located in o Prefrontal, centrotemporal and occipital regions o Cerebellum
		Older vs. Younger individuals	• Decrease in K in few nodes within centrotemporal and occipital regions, and cerebellum • Increase in K and IVI in temporal regions • Increase in C_C in frontal and parietotemporal regions, and cerebellum
Global level (whole-network)	**SN** **FN**	Older vs. Younger individuals	• Decrease in SW, C_C and E_g • Increase in SW and C_C • Decrease in E_g
Hierarchical (rich-club) level	**SN**	Regardless of age	Nodes with higher rich-club scores were located along the anterior-posterior medial axis of the brain in o Fronto-central and occipital region o Subcortical region o Cerebellum
		Older vs. Younger individuals	• Decrease in rich-club score of nodes in superior frontal gyri and cerebellum • Increase in rich-club scores of nodes in precentral gyri, thalamus, superior temporal gyri and superior occipital gyri
	FN	Regardless of age	Nodes with higher rich-club scores were located in o Frontal, centrotemporal, parietal and occipital regions o Cerebellum
		Older vs. Younger individuals	• Decrease in rich-club score of nodes in the majority of functional rich-club nodes • Increase in rich-club score of nodes in middle temporal gyri
Cross-modal level	**SN**	Regardless of age	Involvement in the structural rich club o High for SCN, CAN, DMN, SMN and CBN o Low for TMN
		Older vs. Younger individuals	• Decrease in within-network rich-club connectivity • Increase in between-network rich-club connectivity • Decrease in rich-club involvement of CBN and DMN • Increase in rich-club involvement of SMN, LAN, and SCN
	FN	Regardless of age	Involvement in the functional rich club o High for SMN, LAN, CAN, VIS, CBN and DMN o Low for LMN
		Older vs. Younger individuals	• Decrease in within-network rich-club connectivity • Decrease in between-network rich-club connectivity • Decrease in rich-club involvement of SMN, DMN, and VIS • Increase in rich-club involvement of TMN

SN: structural network; FN: functional network; RC: Rich Club; K: strength/degree; C_C: clustering coefficient; IVI: integrated value of influence; SW: small-worldness; E_g: global efficiency; Refer to Section 2.2.2.3 for the definition of resting-state networks.

Discussion

In this study, we explored age-related differences in structural and functional rich-club connectivity in a large population of aging individuals. We first used graph theoretical measures to investigate age-related trends in the topology of structural and resting-state functional brain networks using a high-resolution whole-brain functional parcellation including cortical and subcortical structures and cerebellum. We then explored age-related differences in the hierarchical organization of the functional and structural connectome as well as in the rich club interconnecting functional subsystems (RSNs). The structure–function coupling was also assessed across the adult lifespan. Finally, we assessed the vulnerability of the structural and functional brain networks to damage to rich club nodes in different RSNs for each age decile. Our findings indicate age-related differences in the topological properties of the structural brain networks along the medial axis of the brain. The resting-state functional brain networks also exhibited significant topological changes related to aging in prefrontal, centrotemporal, and occipital regions, and the cerebellum. Across the adult lifespan, our findings indicated significant age-related differences in the rich-club contributions of RSNs, especially in individuals older than 70 years.

Age-related differences in topological properties of brain networks

Our results demonstrated significant age-related shifts in the integrity of structural brain networks, characterized by decreased integration (measured by strength) and decreased segregation (measured by clustering coefficient). These changes were particularly prominent in the frontal-occipital regions along the medial axis of the brain and in the cerebellum among older participants. However, several subcortical regions (thalamus, pons, and putamen) and parietal areas exhibited increasing integration and segregation with age, correlating with memory and cognitive decline.

Our results align with previous studies [43,65,84,114] that have reported nonlinear trajectories for global efficiency and small-worldness across the lifespan (9–85 yrs), peaking in the third decade. Contrary to the U-shaped trajectory observed for the clustering coefficient by Zhao et al. [114], our findings indicate a linear decline in the clustering coefficient with age. We observed declining trends for these metrics, with an inverted U-shaped trajectory for global efficiency and a bending point within the fifth decade. Our findings align with previous research on the Cam-CAN cohort [118], demonstrating age-related reductions in the clustering coefficient and global efficiency of structural brain networks.

Age-related differences in local efficiency have been reported in various studies [43,65], revealing higher local efficiency in anterior (frontal and temporal) and lower local efficiency in posterior (parietal and occipital) brain areas in older individuals. In comparison with these findings, our results indicate a decline in strength, local efficiency, and clustering coefficient with age, particularly in frontal-occipital regions along the brain's medial axis and in the cerebellum. Notably, we observed increased clustering coefficient, local efficiency, and/or strength with age in certain subcortical regions (thalamus, pons, and putamen) and parietal regions in older subjects, all of which correlated with cognitive decline in memory and visuospatial and language functions. Age-related differences in structural connectivity are suggested to be due to GM shrinkage, loss of small axon fibers and WM degeneration with aging, leading to a significant reduction in the efficiency of paths between nodes along the anterior-posterior axis of the cortex more significantly in frontal areas due to sparsification [13,77,81].

For resting-state functional networks, our results revealed decreased integration (measured by degree) and increased segregation (measured by clustering coefficient) in the prefrontal, centrotemporal, and occipital regions, as well as the cerebellum among older subjects. In contrast, temporal regions exhibited increases in both strength and clustering coefficient with age. Some regions displayed significant age-related differences in nodal metrics correlated with cognitive decline, particularly in memory. Our findings also indicate an increase in the clustering coefficient of functional networks with age, consistent with other studies [67,80,115]. Our findings align closely with those of Sala-Llonch et al. [80], who reported elevated clustering coefficients for nodes in the frontal and parietal lobes, correlating with diminished performance in verbal and visual memory functions among older adults. Furthermore, our results revealed a substantial increase in clustering coefficients with age, particularly in nodes located in the bilateral frontal, temporal, and parietal regions, as well as the cerebellum. These changes were correlated with declines in memory and cognitive functions, including visuospatial and language abilities.

In previous studies, lower local efficiency has been observed in functional networks among older adults compared to their younger counterparts, despite similar global efficiency [21,42]. Consistent with findings by Sala-Llonch et al. [80], our study revealed a declining trend in global efficiency with age. At the network level, we observed no significant differences in local efficiency between younger and older age groups. However, a few bilateral frontal nodes exhibited significant increases in local efficiency with age.

The partial inconsistencies with other findings [41–43,63,65,80,115] are more likely related to differences in sample size and parcellation scales and schemes. The sample size can critically reduce the statistical power, especially in aging studies dealing with a wide range of ages. In addition, the parcellation scale and scheme should ensure functional homogeneity of brain parcels and spatial continuity [37] as well as the reproducibility and stability of network topological properties [21,38,54,60,114]. To overcome these limitations, we used a large sample size ($n = 619$) uniformly distributed across different age deciles. We also performed high-resolution whole-brain functional parcellation to obtain functionally homogeneous parcels ($n = 1133$) within cortical and subcortical regions, deep gray matter and the cerebellum. However, several other factors could potentially account for these inconsistencies. These may include population differences in factors such as genetics, cultural background, and lifestyle, variations in data acquisition methods (such as imaging equipment, scanning protocols, or data preprocessing steps), and heterogeneity within age groups stemming from individual variations in cognitive and neurological function.

Age-related differences in the structural and functional rich-club organization

In line with previous studies [13,54], our findings support the idea that the rich club serves as a structural backbone interconnecting functional brain communities, or RSNs. Consistent with adult studies [7,30,54], our results indicate that subcortical, cognitive control/attention, and default mode networks prominently participate in the structural rich club, mainly comprising connector hubs irrespective of age. Additionally, networks such as sensory-motor, language, auditory, and cerebellar networks also exhibit involvement in the structural rich club.

Our results identified influential nodes [61], known as spreaders, located in the core of structural brain networks along the medial frontal-occipital axis and within subcortical regions and the cerebellum. With the exception of subcortical areas, the spreading potential of these nodes significantly decreased, especially in individuals older than 70 years. Additionally, in structural networks, our findings indicated a decrease in the involvement of the cerebellum and DMN in the rich club with age. Conversely, sensory-motor, language-auditory, and subcortical networks exhibited an opposite trend, reflecting an age-related redistribution of rich-club nodes. Notably, our results align with other studies [23,107] demonstrating an age-related increase in the structural connectivity of subcortical regions.

Structural brain networks exhibiting age-related decreases in connectivity are primarily composed of association fibers connecting regions within the same hemisphere. Conversely, networks showing age-related increases in connectivity, such as the subcortical network, are predominantly composed of commissural fibers connecting the two hemispheres [12,87]. According to the last-in-first-out hypothesis, association fibers, which exhibit a later peak of maturation, are suggested to be more susceptible to age-related decline compared to commissural fibers [49].

Consistent with prior network studies [13,45], our results revealed that the majority of intra-RSN (within) and inter-RSN (between) structural rich-club connections—known for efficiently integrating functionally segregated brain regions—were long-distance, exceeding 70 mm for structural networks and 50 mm for functional networks, across all age deciles. Notably, the cerebellum exhibited persistent segregation across age groups, with nearly 68 % of its connections remaining within-module and short-distance. In contrast, the subcortical network demonstrated higher integration potential, with almost 60 % of its inter-RSN connections spanning long distances across the entire brain network.

However, our investigation revealed age-related trends in the proportion of intra- and inter-RSN rich-club connections. We observed an increasing trend in intra-RSN connections and a decreasing trend in inter-RSN connections with age. Interestingly, irrespective of age, our findings showed that the majority of connections within DMN, SCN, and LMN were long-distance. Conversely, for other RSNs, almost one-third of intra- and inter-RSN connections were short-range (RC, feeder, and local). Consistent with prior research [21], our results suggest that the proportion of short- and long-distance connections undergoes changes with age, indicative of a significant reduction in communication and total network cost associated with the aging process [102].

We also examined the age-related redistribution of functional rich club nodes in different RSNs. Our results showed that SMN (predominantly) as well as LAN, CAN, VIS, CBN and DMN were largely involved in the functional rich club in older individuals, in line with other functional connectivity studies [47,51].

In studies conducted using the Cam-CAN cohort [71,106], an age-related decrease in functional connectivity of the default mode network and visual network was observed, aligning with our findings. Overall, our results suggest that the age-related redistribution of rich-club nodes may differ between structural and functional brain networks. However, consistent age-related decreases in RC involvement in the default mode network and cerebellum were observed in both networks.

Extensive research has investigated age-related changes in brain network segregation and integration, focusing on both structural and functional networks (for a review see [33]. Our study contributes to the existing literature by specifically examining rich club connectivity within and between networks. In contrast to other studies that have focused on between-network connectivity of specific RSN pairs, our emphasis was on age-related changes in rich club connectivity between each RSN and all other RSNs across the entire brain. Our analysis revealed that, in structural networks, between-network RC connectivity increased in older subjects, while within-network RC connectivity decreased in older age groups. Conversely, in functional networks, both between-network and within-network RC connectivity decreased in older subjects. These findings align with existing literature indicating a decline in within-network connectivity and an increase in between-network connectivity with age [13,44,56,74,93].

Our findings further revealed subtle yet distinct age-related trends. Specifically, we observed a decrease in within-network connectivity and an increase in between-network connectivity for DMN and SMN using structural connectivity analysis. Similarly, this trend was noted in CAN, DMN and LAN through functional connectivity analysis. Several studies have reported similar trends in DMN and SMN [63,71,93,99,105–106,118], and CAN [21–22,57]. Overall, findings across different functional studies regarding age-related changes in within-network connectivity are more heterogeneous for sensory and motor networks in comparison with higher-order functional networks such as the default mode, fronto-parietal, executive control, and cingulo-opercular networks. This observed pattern aligns with a 'last-in-first-out' configuration during maturation, suggesting that later-maturing higher-order brain regions are more susceptible to earlier age-related decline [63].

Cross-age rich club regions

Largely consistent with other studies [21,45,47,54,114], we found several high-degree structural rich-club regions mostly distributed along the medial axis of the brain, in deep structures (pons, putamen, thalamus, caudate), cerebellum, frontal regions (superior and middle frontal and precentral gyri), insula, anterior cingulate gyrus, median cingulate and paracingulate gyri, supplementary motor area, paracentral lobule, superior temporal gyrus, parietal regions (precuneus) and occipital regions (superior occipital gyrus). Among these regions, the superior frontal gyri and cerebellum exhibited RC scores decreasing with age, especially in

individuals older than 70 years. Zhao et al. [114] also reported the loss of frontal hubs and their connections due to the aging process. Unique to this sample, we found an age-related decrease in the RC score of the cerebellum along with the aging decline in cognitive performance. This may be due to the loss of connections between the cerebellum, motor, and cognitive cortical regions reported in other studies [34,92]. Our results also showed that the RC scores of a few brain regions including the precentral gyri, thalamus, superior temporal gyri and superior occipital gyri increased with age, mainly because of the redistribution of the top 30 % of RC nodes across different age deciles.

In functional networks, our results indicated that high-degree RC nodes were primarily situated on the outer surface of the cortex, specifically in centrotemporal and occipital areas, encompassing the precentral and postcentral gyri, insula, frontal regions, middle and superior temporal gyri, occipital regions, and cerebellum. This distribution is partially consistent with findings from other studies [21,45]. We observed a significant age-related reduction in RC scores across nearly all functional RC regions, particularly in individuals older than 70 years. However, an exception was noted for those located in the bilateral middle temporal gyri, which gained priority in the functional rich club due to the functional RC reorganization in older individuals.

Age-related differences in structure–function coupling

Several studies have assessed age-related differences in coupling between structural and functional connectivity in healthy populations, reporting correlations with varying degrees between 0.3 and 0.7 [94,116]. Our results also showed a structure–function correlation lower than 0.21, linearly declining ($r = -0.38$) with age, in line with other findings [112,116]. The discordance between structural and functional connectivity is shown to be more heterogeneous in RSNs at the macroscopic level, more likely due to functional interactions through indirect structural connections resulting in partial correspondence between structural and functional connectivity [14,70]. In a few studies [11,73,75,104], higher SFC has been reported in unimodal sensory and motor cortices like sensory-motor, visual and auditory networks in comparison with transmodal association cortices like limbic and default mode networks. Esfahlani et al. [112] have found a decreasing trend for SFC with age in sensorimotor systems in comparison with higher-order cognitive systems exhibiting SFC preserved across the lifespan. Our results also revealed a significant reduction in SFC with age for SMN as well as for CBN, CAN, and SCN. In contrast with the findings reported by Zamani Esfahlani et al. [112], we found an age-related decline in SFC with age for DMN and TMN, however, with a lower declining rate in comparison with sensorimotor cortices. In our results, no age-related differences in SFC were observed in auditory, language, visual and limbic systems.

We also investigated age-related coupling between nodal measures (degree, clustering coefficient and local efficiency) of the structural and functional brain networks. The age-related differences in SFC based on nodal metrics were much less heterogeneous and significant than those found between functional and structural connection strengths. Our results indicated rather a weak coupling (<0.1) between whole-brain functional/structural nodal degree, local efficiency and clustering coefficient, slightly decreasing with age. Among all RSNs, the coupling between the structural and functional degree decreased for nodes within LMN and CBN with age. Only within LAN, the SFC between the nodal degree and efficiency increased with age.

Overall, the imperfect SFC and the heterogeneity of age-related differences in SFC are suggested to be due to regional and inter-individual variability, global organizational differences between structural and functional networks, functional interactions through indirect structural connections, regional heterogeneity, higher-order interactions among functional regions, and modulating structure–function relationships [94,112].

Age-related differences in network vulnerability to loss of RC nodes

In adults, previous studies have demonstrated the vulnerability of structural networks to the loss of rich club nodes, suggested to be due to the central role of RC hubs in integrating neural information between brain regions [26,102]. We investigated the effect of damage to structural and functional RC nodes within each RSN on the network efficiency in different age deciles. While we observed a slight decrease in global efficiency with age, particularly in the last two aging groups (as indicated in Table 2), cross-age differences in the vulnerability index—a relative metric reflecting the percentage change in global efficiency of the entire brain's structural/functional network after the removal of rich club nodes—were found to be specific to RSNs. Our results showed higher structural vulnerability to loss of RC nodes within LAN, VIS and SCN, decreasing with age. The network vulnerability to damage to RC nodes in CBN, TMN and SCN, however, increased with age more likely due to their increased structural connectivity, especially for SCN [23]. For the functional networks, our study indicates higher network vulnerability to attacks on RC nodes in CBN, LAN and SMN. Interestingly, the functional networks showed more resilience to damage to RC nodes in DMN and LMN. The vulnerability analysis also showed less vulnerability for functional networks to attack on RC connectivity in CBN, DMN, SCN and TMN at older ages. Previous studies have reported both lower and higher vulnerability of brain networks at older ages [9,36]. Overall, our findings support previous research suggesting that disease-related damage to the structural RC connectivity affecting global communication processes may not proportionally affect brain functioning, specifically the higher-order cognitive processes which highly depend on the global integration of information [54]. Overall, the vulnerability analysis provided a better understanding of how focal damage could disrupt the rich club connectivity in structural and functional brain networks. Further investigation is required to assess the extent to which the damage to hub brain regions can result in cognitive impairment in neurological disorders with foal brain lesions.

Limitations

Due to the large number of exploratory analyses performed in this study, the effect of some parameters on connectivity results was

not investigated. First, the potential effect of gender, brain volume and education should be modeled in the regression analysis as they may affect affect derived connectivity measures [32]. Second, there are age-specific parcellation schemes introduced in other studies [48]. In comparison to groupwise parcellation schemes, age-specific parcellation schemes are posited to offer a more nuanced representation of the aging brain. Thirdly, our selection of a high-resolution parcellation scheme, which subdivides the brain into smaller regions, may potentially lead to a reduction in the signal-to-noise ratio (SNR). Thus, it is crucial to thoroughly examine SNRs across different parcellation scales and assess their impact on the reliability of connectivity outcomes. Finally, the thresholding approach can affect the density of connections and network topology leading to unreliable results. The use of multiple thresholds or fully-weighted networks can better illustrate the sensitivity of network topology to the thresholding process [86]. Future investigations are required to address these limitations.

Conclusion

In this study, we explored age-related differences in structural and functional brain connectivity using the graph theoretical analysis from regional and global perspectives. Our findings indicate that the cognitive control/attention, default mode, sensory-motor, language-auditory and subcortical networks as well as the cerebellum were involved in both the structural and functional rich club. The rich-club involvement of the default mode network and cerebellum decreased significantly in individuals older than 70 years old. We found reduced integration and segregation within the frontal-occipital regions and the cerebellum along the brain's medial axis in older subjects. Additionally, functional brain networks in older particiapnts exhibited reduced integration and increased segregation in the prefrontal, centrotemporal, occipital regions, and cerebellum. Furthermore, we observed a decline in within-network RC connectivity and an increase in between-network RC connectivity in structural networks among older individuals. Additionally, both within-network and between-network RC connectivity diminished in functional networks with age. A significant reduction in structure–function coupling was observed with age within the sensory-motor, cognitive-attention and subcortical networks. The structural network vulnerability was higher to the loss of RC nodes within the language-auditory, visual and subcortical networks. For the functional networks, our study indicated a greater vulnerability to attacks on RC nodes in the cerebellum, language-auditory and sensory-motor networks. Overall, the network vulnerability decreased significantly in subjects aged 70 and older in both networks. These findings collectively contribute to a deeper understanding of the impact of age on the integrity of functional and structural brain networks, shedding light on vulnerabilities and patterns. This knowledge can inform future research, particularly investigations into the effects of local structural damage on RC connectivity between brain networks, especially in aging populations.

Data availability statement

Data used in the preparation of this work were obtained from the CamCAN repository (available at https://www.mrc-cbu.cam.ac.uk/datasets/camcan/), [83,95].

CRediT authorship contribution statement

Maedeh Khalilian: Data curation, Formal analysis, Investigation, Methodology, Visualization, Writing – original draft, Writing – review & editing. **Monica N. Toba:** Writing – review & editing, Supervision. **Martine Roussel:** Writing – review & editing. **Sophie Tasseel-Ponche:** Writing – review & editing. **Olivier Godefroy:** Writing – review & editing. **Ardalan Aarabi:** Conceptualization, Supervision, Investigation, Methodology, Writing – review & editing.

Declaration of competing interest

The authors declare that they have no known competing financial interests or personal relationships that could have appeared to influence the work reported in this paper.

Acknowledgments

"Data collection and sharing for this project was provided by the Cambridge Centre for Ageing and Neuroscience (CamCAN). CamCAN funding was provided by the UK Biotechnology and Biological Sciences Research Council (grant number BB/H008217/1), together with support from the UK Medical Research Council and University of Cambridge, UK".

Appendix A. Supplementary data

Supplementary data to this article can be found online at https://doi.org/10.1016/j.nbas.2023.100105.

References

[1] Aerts H, Fias W, Caeyenberghs K, Marinazzo D. Brain networks under attack: robustness properties and the impact of lesions. Brain J Neurol 2016;139: 3063–83. https://doi.org/10.1093/brain/aww194.
[2] Ahmadi M, Kazemi K, Kuc K, Cybulska-Klosowicz A, Helfroush MS, Aarabi A. Resting state dynamic functional connectivity in children with attention deficit/ hyperactivity disorder. J Neural Eng 2021;18. https://doi.org/10.1088/1741-2552/ac16b3.
[3] Allen EA, Erhardt EB, Damaraju E, Gruner W, Segall JM, Silva RF, et al. A baseline for the multivariate comparison of resting-state networks. Front Syst Neurosci 2011;5:2.
[4] Andersson JLR, Graham MS, Zsoldos E, Sotiropoulos SN. Incorporating outlier detection and replacement into a non-parametric framework for movement and distortion correction of diffusion MR images. Neuroimage 2016;141:556–72. https://doi.org/10.1016/j.neuroimage.2016.06.058.
[5] Andersson JLR, Sotiropoulos SN. An integrated approach to correction for off-resonance effects and subject movement in diffusion MR imaging. Neuroimage 2016;125:1063–78. https://doi.org/10.1016/j.neuroimage.2015.10.019.
[6] Andrews-Hanna JR, Snyder AZ, Vincent JL, Lustig C, Head D, Raichle ME, et al. Disruption of large-scale brain systems in advanced aging. Neuron 2007;56: 924–35.
[7] Arcaro MJ, Livingstone MS. A hierarchical, retinotopic proto-organization of the primate visual system at birth. Elife 2017;6:e26196.
[8] Bassett DS, Bullmore ET, Meyer-Lindenberg A, Apud JA, Weinberger DR, Coppola R. Cognitive fitness of cost-efficient brain functional networks. Proc Natl Acad Sci 2009;106:11747–52. https://doi.org/10.1073/pnas.0903641106.
[9] Bassignana G, Lacidogna G, Bartolomeo P, Colliot O, De Vico Fallani F. The impact of aging on human brain network target controllability. Brain Struct Funct 2022;227:3001–15. https://doi.org/10.1007/s00429-022-02584-w.
[10] Bastiani M, Andersson JLR, Cordero-Grande L, Murgasova M, Hutter J, Price AN, et al. Automated processing pipeline for neonatal diffusion MRI in the developing Human Connectome Project. Neuroimage 2019;185:750–63. https://doi.org/10.1016/j.neuroimage.2018.05.064.
[11] Baum GL, Cui Z, Roalf DR, Ciric R, Betzel RF, Larsen B, et al. Development of structure–function coupling in human brain networks during youth. Proc Natl Acad Sci 2020;117:771–8. https://doi.org/10.1073/pnas.1912034117.
[12] Bender AR, Völkle MC, Raz N. Differential aging of cerebral white matter in middle-aged and older adults: a seven-year follow-up. Neuroimage 2016;125: 74–83. https://doi.org/10.1016/j.neuroimage.2015.10.030.
[13] Betzel RF, Byrge L, He Y, Goñi J, Zuo X-N, Sporns O. Changes in structural and functional connectivity among resting-state networks across the human lifespan. Neuroimage 2014;102(Pt 2):345–57. https://doi.org/10.1016/j.neuroimage.2014.07.067.
[14] Betzel RF, Medaglia JD, Bassett DS. Diversity of meso-scale architecture in human and non-human connectomes. Nat Commun 2018;9:346. https://doi.org/10.1038/s41467-017-02681-z.
[15] Bialystok E, Craik FIM, editors. Lifespan Cognition: Mechanisms of Change. New York: Oxford University Press; 2006. https://doi.org/10.1093/acprof:oso/9780195169539.001.0001.
[16] Biswal BB, Mennes M, Zuo X-N, Gohel S, Kelly C, Smith SM, et al. Toward discovery science of human brain function. Proc Natl Acad Sci USA 2010;107: 4734–9. https://doi.org/10.1073/pnas.0911855107.
[17] Book Series: Handbook of Clinical Neurology [WWW Document], n.d. URL: https://www.elsevier.com/books/book-series/handbook-of-clinical-neurology (accessed 8.30.21).
[18] Braun U, Plichta MM, Esslinger C, Sauer C, Haddad L, Grimm O, et al. Test-retest reliability of resting-state connectivity network characteristics using fMRI and graph theoretical measures. Neuroimage 2012;59:1404–12. https://doi.org/10.1016/j.neuroimage.2011.08.044.
[19] Bullmore E, Sporns O. Complex brain networks: graph theoretical analysis of structural and functional systems. Nat Rev Neurosci 2009;10:186–98. https://doi.org/10.1038/nrn2575.
[20] Calhoun VD, Adali T, Pearlson G, Pekar J. Group ICA of functional MRI data: separability, stationarity, and inference. In Proc. Int. Conf. on ICA and BSS San Diego, CA; 2001.
[21] Cao M, Wang J-H, Dai Z-J, Cao X-Y, Jiang L-L, Fan F-M, et al. Topological organization of the human brain functional connectome across the lifespan. Dev Cogn Neurosci 2014;7:76–93. https://doi.org/10.1016/j.dcn.2013.11.004.
[22] Chan MY, Park DC, Savalia NK, Petersen SE, Wig GS. Decreased segregation of brain systems across the healthy adult lifespan. Proc Natl Acad Sci 2014;111: E4997–5006. https://doi.org/10.1073/pnas.1415122111.
[23] Coelho A, Fernandes HM, Magalhães R, Moreira PS, Marques P, Soares JM, et al. Reorganization of brain structural networks in aging: a longitudinal study. J Neurosci Res 2021;99:1354–76. https://doi.org/10.1002/jnr.24795.
[24] Cole DM, Smith SM, Beckmann CF. Advances and pitfalls in the analysis and interpretation of resting-state FMRI data. Front Syst Neurosci 2010;4:8. https://doi.org/10.3389/fnsys.2010.00008.
[25] Colizza V, Flammini A, Serrano MA, Vespignani A. Detecting rich-club ordering in complex networks. Nat Phys 2006;2:110–5. https://doi.org/10.1038/nphys209.
[26] Collin G, Sporns O, Mandl RCW, Van Den Heuvel MP. Structural and functional aspects relating to cost and benefit of rich club organization in the human cerebral cortex. Cereb Cortex 2014;24:2258–67. https://doi.org/10.1093/cercor/bht064.
[27] Collin G, van den Heuvel MP. The ontogeny of the human connectome: development and dynamic changes of brain connectivity across the life span. Neurosci Rev J Bringing Neurobiol Neurol Psychiatry 2013;19:616–28. https://doi.org/10.1177/1073858413503712.
[28] Cox RW. AFNI: software for analysis and visualization of functional magnetic resonance neuroimages. Comput Biomed Res 1996;29:162–73.
[29] Craddock RC, James GA, Holtzheimer PE, Hu XP, Mayberg HS. A whole brain fMRI atlas generated via spatially constrained spectral clustering. Hum Brain Mapp 2012;33:1914–28. https://doi.org/10.1002/hbm.21333.
[30] Dall'Orso S, Steinweg J, Allievi AG, Edwards AD, Burdet E, Arichi T. Somatotopic mapping of the developing sensorimotor cortex in the preterm human brain. Cereb Cortex N Y N 2018;1991(28):2507–15. https://doi.org/10.1093/cercor/bhy050.
[31] Damaraju E, Allen EA, Belger A, Ford JM, McEwen S, Mathalon DH, et al. Dynamic functional connectivity analysis reveals transient states of dysconnectivity in schizophrenia. NeuroImage Clin 2014;5:298–308.
[32] Damoiseaux JS. Effects of aging on functional and structural brain connectivity. Neuroimage 2017;160:32–40. https://doi.org/10.1016/j.neuroimage.2017.01.077.
[33] Deery HA, Di Paolo R, Moran C, Egan GF, Jamadar SD. The older adult brain is less modular, more integrated, and less efficient at rest: a systematic review of large-scale resting-state functional brain networks in aging. Psychophysiology 2023;60:e14159.
[34] Dum RP, Levinthal DJ, Strick PL. The spinothalamic system targets motor and sensory areas in the cerebral cortex of monkeys. J Neurosci Off J Soc Neurosci 2009;29:14223–35. https://doi.org/10.1523/JNEUROSCI.3398-09.2009.
[35] Ferreira LK, Busatto GF. Resting-state functional connectivity in normal brain aging. Neurosci Biobehav Rev 2013;37:384–400. https://doi.org/10.1016/j.neubiorev.2013.01.017.
[36] Filippi M, Cividini C, Basaia S, Spinelli EG, Castelnovo V, Leocadi M, et al. Age-related vulnerability of the human brain connectome. Mol Psychiatry 2023;1–9. https://doi.org/10.1038/s41380-023-02157-1.
[37] Fornito A, Zalesky A, Breakspear M. Graph analysis of the human connectome: promise, progress, and pitfalls. Neuroimage 2013;80:426–44. https://doi.org/10.1016/j.neuroimage.2013.04.087.
[38] Fouladivanda M, Kazemi K, Makki M, Khalilian M, Danyali H, Gervain J, et al. Multi-scale structural rich-club organization of the brain in full-term newborns: a combined DWI and fMRI study. J Neural Eng 2021;18. https://doi.org/10.1088/1741-2552/abfd46.
[39] Freeman LC. Centrality in social networks conceptual clarification. Soc Netw 1978;1:215–39. https://doi.org/10.1016/0378-8733(78)90021-7.
[40] Friston KJ, Ashburner J, Frith CD, Poline J, Heather JD, Frackowiak RSJ. Spatial registration and normalization of images. Hum Brain Mapp 1995;3:165–89.
[41] Galluzzi S, Beltramello A, Filippi M, Frisoni GB. Aging Neurol Sci 2008;29(Suppl 3):296–300. https://doi.org/10.1007/s10072-008-1002-6.

[42] Geerligs L, Renken RJ, Saliasi E, Maurits NM, Lorist MM. A brain-wide study of age-related changes in functional connectivity. Cereb Cortex N Y N 2015;1991 (25):1987–99. https://doi.org/10.1093/cercor/bhu012.
[43] Gong G, Rosa-Neto P, Carbonell F, Chen ZJ, He Y, Evans AC. Age- and gender-related differences in the cortical anatomical network. J Neurosci 2009;29: 15684–93. https://doi.org/10.1523/JNEUROSCI.2308-09.2009.
[44] Grady C, Sarraf S, Saverino C, Campbell K. Age differences in the functional interactions among the default, frontoparietal control, and dorsal attention networks. Neurobiol Aging 2016;41:159–72. https://doi.org/10.1016/j.neurobiolaging.2016.02.020.
[45] Grayson DS, Ray S, Carpenter S, Iyer S, Dias TGC, Stevens C, et al. Structural and functional rich club organization of the brain in children and adults. PLoS One 2014;9:e88297.
[46] Guimerà R, Nunes Amaral LA. Functional cartography of complex metabolic networks. Nature 2005;433:895–900. https://doi.org/10.1038/nature03288.
[47] Hagmann P, Cammoun L, Gigandet X, Meuli R, Honey CJ, Wedeen VJ, et al. Mapping the structural core of human cerebral cortex. PLOS Biol 2008;6:e159.
[48] Han L, Savalia NK, Chan MY, Agres PF, Nair AS, Wig GS. Functional parcellation of the cerebral cortex across the human adult lifespan. Cereb Cortex N Y N 2018;1991(28):4403–23. https://doi.org/10.1093/cercor/bhy218.
[49] Hermoye L, Saint-Martin C, Cosnard G, Lee S-K, Kim J, Nassogne M-C, et al. Pediatric diffusion tensor imaging: normal database and observation of the white matter maturation in early childhood. Neuroimage 2006;29:493–504. https://doi.org/10.1016/j.neuroimage.2005.08.017.
[50] Herrero M-T, Barcia C, Navarro JM. Functional anatomy of thalamus and basal ganglia. Childs Nerv Syst 2002;18:386–404. https://doi.org/10.1007/s00381-002-0604-1.
[51] van den Heuvel M, Mandl R, Luigjes J, Pol HH. Microstructural organization of the cingulum tract and the level of default mode functional connectivity. J Neurosci 2008;28:10844–51. https://doi.org/10.1523/JNEUROSCI.2964-08.2008.
[52] van den Heuvel M, Mandl R, Pol HH. Normalized cut group clustering of resting-state fMRI data. PLoS One 2008;3:e2001.
[53] van den Heuvel MP, Sporns O. An anatomical substrate for integration among functional networks in human cortex. J Neurosci 2013;33:14489–500. https://doi.org/10.1523/JNEUROSCI.2128-13.2013.
[54] van den Heuvel MP, Sporns O. Rich-club organization of the human connectome. J Neurosci 2011;31:15775–86. https://doi.org/10.1523/JNEUROSCI.3539-11.2011.
[55] Honey CJ, Sporns O, Cammoun L, Gigandet X, Thiran JP, Meuli R, et al. Predicting human resting-state functional connectivity from structural connectivity. Proc Natl Acad Sci 2009;106:2035–40. https://doi.org/10.1073/pnas.0811168106.
[56] Hou X, Liu P, Gu H, Chan M, Li Y, Peng S-L, et al. Estimation of brain functional connectivity from hypercapnia BOLD MRI data: validation in a lifespan cohort of 170 subjects. Neuroimage 2019;186:455–63. https://doi.org/10.1016/j.neuroimage.2018.11.028.
[57] Jenkinson M, Bannister P, Brady M, Smith S. Improved optimization for the robust and accurate linear registration and motion correction of brain images. Neuroimage 2002;17:825–41.
[58] Jenkinson M, Smith S. A global optimisation method for robust affine registration of brain images. Med Image Anal 2001;5:143–56.
[59] Kesler SR, Watson CL, Blayney DW. Brain network alterations and vulnerability to simulated neurodegeneration in breast cancer. Neurobiol Aging 2015;36: 2429–42. https://doi.org/10.1016/j.neurobiolaging.2015.04.015.
[60] Khalilian M, Kazemi K, Fouladivanda M, Makki M, Helfroush MS, Aarabi A. Effect of Multishell diffusion MRI acquisition strategy and parcellation scale on rich-club organization of human brain structural networks. Diagn Basel Switz 2021;11:970. https://doi.org/10.3390/diagnostics11060970.
[61] Kitsak M, Gallos LK, Havlin S, Liljeros F, Muchnik L, Stanley HE, et al. Identification of influential spreaders in complex networks. Nat Phys 2010;6:888–93. https://doi.org/10.1038/nphys1746.
[62] Liem F, Geerligs L, Damoiseaux JS, Margulies DS. Chapter 3 – Functional connectivity in aging. In: Schaie KW, Willis SL, editors. Handbook of the Psychology of Aging (Ninth Edition), Handbooks of Aging. Academic Press; 2021. p. 37–51. https://doi.org/10.1016/B978-0-12-816094-7.00010-6.
[63] Luo N, Sui J, Abrol A, Lin D, Chen J, Vergara VM, et al. Age-related structural and functional variations in 5,967 individuals across the adult lifespan. Hum Brain Mapp 2019;41:1725–37. https://doi.org/10.1002/hbm.24905.
[64] Madden DJ, Bennett IJ, Burzynska A, Potter GG, Chen N-K, Song AW. Diffusion tensor imaging of cerebral white matter integrity in cognitive aging. Biochim Biophys Acta 2012;1822:386–400. https://doi.org/10.1016/j.bbadis.2011.08.003.
[65] Madden DJ, Jain S, Monge ZA, Cook AD, Lee A, Huang H, et al. Influence of structural and functional brain connectivity on age-related differences in fluid cognition. Neurobiol Aging 2020;96:205–22. https://doi.org/10.1016/j.neurobiolaging.2020.09.010.
[66] Maffei C, Sarubbo S, Jovicich J. Diffusion-based tractography atlas of the human acoustic radiation. Sci Rep 2019;9:4046. https://doi.org/10.1038/s41598-019-40666-8.
[67] Matthäus F, Schmidt J-P, Banerjee A, Schulze TG, Demirakca T, Diener C. Effects of age on the structure of functional connectivity networks during episodic and working memory demand. Brain Connect 2012;2:113–24. https://doi.org/10.1089/brain.2012.0077.
[68] Meier J, Tewarie P, Hillebrand A, Douw L, van Dijk BW, Stufflebeam SM, et al. A mapping between structural and functional brain networks. Brain Connect 2016;6:298–311. https://doi.org/10.1089/brain.2015.0408.
[69] Mioshi E, Dawson K, Mitchell J, Arnold R, Hodges JR. The Addenbrooke's Cognitive Examination Revised (ACE-R): a brief cognitive test battery for dementia screening. Int J Geriatr Psychiatry 2006;21:1078–85. https://doi.org/10.1002/gps.1610.
[70] Mišić B, Betzel RF, Nematzadeh A, Goñi J, Griffa A, Hagmann P, et al. Cooperative and competitive spreading dynamics on the human connectome. Neuron 2015;86:1518–29. https://doi.org/10.1016/j.neuron.2015.05.035.
[71] Monti RP, Gibberd A, Roy S, Nunes M, Lorenz R, Leech R, et al. Interpretable brain age prediction using linear latent variable models of functional connectivity. PLoS One 2020;15:e0232296.
[72] Otsu N. A threshold selection method from gray-level histograms. IEEE Trans Syst Man Cybern 1979;9:62–6. https://doi.org/10.1109/TSMC.1979.4310076.
[73] Paquola C, Wael RVD, Wagstyl K, Bethlehem RAI, Hong S-J, Seidlitz J, et al. Microstructural and functional gradients are increasingly dissociated in transmodal cortices. PLOS Biol 2019;17:e3000284.
[74] Pedersen R, Geerligs L, Andersson M, Gorbach T, Avelar-Pereira B, Wåhlin A, et al. When functional blurring becomes deleterious: reduced system segregation is associated with less white matter integrity and cognitive decline in aging. Neuroimage 2021;242:118449. https://doi.org/10.1016/j.neuroimage.2021.118449.
[75] Preti MG, Van De Ville D. Decoupling of brain function from structure reveals regional behavioral specialization in humans. Nat Commun 2019;10:4747. https://doi.org/10.1038/s41467-019-12765-7.
[76] Ramanoël S, Hoyau E, Kauffmann L, Renard F, Pichat C, Boudiaf N, et al. Gray matter volume and cognitive performance during normal aging. A voxel-based morphometry study. Front Aging Neurosci 2018;10.
[77] Raz N, Gunning FM, Head D, Dupuis JH, McQuain J, Briggs SD, et al. Selective aging of the human cerebral cortex observed in vivo: differential vulnerability of the prefrontal gray matter. Cereb Cortex N Y N 1997;1991(7):268–82. https://doi.org/10.1093/cercor/7.3.268.
[78] Ridwan AR, Niaz MR, Wu Y, Qi X, Zhang S, Kontzialis M, et al. Development and evaluation of a high performance T1-weighted brain template for use in studies on older adults. Hum Brain Mapp 2021;42:1758–76. https://doi.org/10.1002/hbm.25327.
[79] Rueckert D, Sonoda LI, Hayes C, Hill DLG, Leach MO, Hawkes DJ. Nonrigid registration using free-form deformations: application to breast MR images. IEEE Trans Med Imaging 1999;18:712–21.
[80] Sala-Llonch R, Junqué C, Arenaza-Urquijo EM, Vidal-Piñeiro D, Valls-Pedret C, Palacios EM, et al. Changes in whole-brain functional networks and memory performance in aging. Neurobiol Aging 2014;35:2193–202. https://doi.org/10.1016/j.neurobiolaging.2014.04.007.
[81] Salat D, Lee S, van der Kouwe A, Greve D, Fischl B, Rosas H. Age-associated alterations in cortical gray and white matter signal intensity and gray to white matter contrast. Neuroimage 2009;48:21–8. https://doi.org/10.1016/j.neuroimage.2009.06.074.
[82] Salavaty A, Ramialison M, Currie PD. Integrated value of influence: an integrative method for the identification of the most influential nodes within networks. Patterns N Y N 2020;1:100052. https://doi.org/10.1016/j.patter.2020.100052.

[83] Shafto MA, Tyler LK, Dixon M, Taylor JR, Rowe JB, Cusack R, et al. The Cambridge Centre for Ageing and Neuroscience (Cam-CAN) study protocol: a cross-sectional, lifespan, multidisciplinary examination of healthy cognitive ageing. BMC Neurol 2014;14:204. https://doi.org/10.1186/s12883-014-0204-1.
[84] Shah C, Liu J, Lv P, Sun H, Xiao Y, Liu J, et al. Age related changes in topological properties of brain functional network and structural connectivity. Front Neurosci 2018;12. https://doi.org/10.3389/fnins.2018.00318.
[85] Shaw P, Kabani NJ, Lerch JP, Eckstrand K, Lenroot R, Gogtay N, et al. Neurodevelopmental trajectories of the human cerebral cortex. J Neurosci 2008;28:3586–94. https://doi.org/10.1523/JNEUROSCI.5309-07.2008.
[86] Simpson SL, Bowman FD, Laurienti PJ. Analyzing complex functional brain networks: fusing statistics and network science to understand the brain. Stat Surv 2013;7:1–36. https://doi.org/10.1214/13-SS103.
[87] Slater DA, Melie-Garcia L, Preisig M, Kherif F, Lutti A, Draganski B. Evolution of white matter tract microstructure across the life span. Hum Brain Mapp 2019;40:2252–68. https://doi.org/10.1002/hbm.24522.
[88] Sowell ER, Thompson PM, Leonard CM, Welcome SE, Kan E, Toga AW. Longitudinal mapping of cortical thickness and brain growth in normal children. J Neurosci Off J Soc Neurosci 2004;24:8223–31. https://doi.org/10.1523/JNEUROSCI.1798-04.2004.
[89] Sporns O, Honey CJ, Kötter R. Identification and classification of hubs in brain networks. PLoS One 2007;2:e1049.
[90] Sporns O, Tononi G, Kötter R. The human connectome: a structural description of the human brain. PLOS Comput Biol 2005;1:e42.
[91] Spreng RN, Stevens WD, Viviano JD, Schacter DL. Attenuated anticorrelation between the default and dorsal attention networks with aging: Evidence from task and rest. Neurobiol Aging 2016;45:149–60. https://doi.org/10.1016/j.neurobiolaging.2016.05.020.
[92] Strick PL, Dum RP, Fiez JA. Cerebellum and nonmotor function. Annu Rev Neurosci 2009;32:413–34. https://doi.org/10.1146/annurev.neuro.31.060407.125606.
[93] Stumme J, Jockwitz C, Hoffstaedter F, Amunts K, Caspers S. Functional network reorganization in older adults: graph-theoretical analyses of age, cognition and sex. Neuroimage 2020;214:116756. https://doi.org/10.1016/j.neuroimage.2020.116756.
[94] Suárez LE, Markello RD, Betzel RF, Misic B. Linking structure and function in macroscale brain networks. Trends Cogn Sci 2020;24:302–15. https://doi.org/10.1016/j.tics.2020.01.008.
[95] Taylor JR, Williams N, Cusack R, Auer T, Shafto MA, Dixon M, et al. The Cambridge Centre for Ageing and Neuroscience (Cam-CAN) data repository: structural and functional MRI, MEG, and cognitive data from a cross-sectional adult lifespan sample. NeuroImage Data Sharing Part II 2017;144:262–9. https://doi.org/10.1016/j.neuroimage.2015.09.018.
[96] Termenon M, Achard S, Jaillard A, Delon-Martin C. The "Hub Disruption Index", a reliable index sensitive to the brain networks reorganization. A study of the contralesional hemisphere in stroke. Front Comput Neurosci 2016;10:84. https://doi.org/10.3389/fncom.2016.00084.
[97] Terribilli D, Schaufelberger MS, Duran FLS, Zanetti MV, Curiati PK, Menezes PR, et al. Age-related gray matter volume changes in the brain during non-elderly adulthood. Neurobiol Aging 2011;32:354–68. https://doi.org/10.1016/j.neurobiolaging.2009.02.008.
[98] Thomas Yeo BT, Krienen FM, Sepulcre J, Sabuncu MR, Lashkari D, Hollinshead M, et al. The organization of the human cerebral cortex estimated by intrinsic functional connectivity. J Neurophysiol 2011;106:1125–65. https://doi.org/10.1152/jn.00338.2011.
[99] Tomasi D, Volkow ND. Aging and functional brain networks. Mol Psychiatry 2012;17(471):549–58. https://doi.org/10.1038/mp.2011.81.
[100] Tzourio-Mazoyer N, Landeau B, Papathanassiou D, Crivello F, Etard O, Delcroix N, et al. Automated anatomical labeling of activations in SPM using a macroscopic anatomical parcellation of the MNI MRI single-subject brain. Neuroimage 2002;15:273–89. https://doi.org/10.1006/nimg.2001.0978.
[101] van den Heuvel MP, Hulshoff Pol HE. Exploring the brain network: a review on resting-state fMRI functional connectivity. Eur Neuropsychopharmacol J Eur Coll Neuropsychopharmacol 2010;20:519–34. https://doi.org/10.1016/j.euroneuro.2010.03.008.
[102] Van den Heuvel MP, Kahn RS, Goñi J, Sporns O. High-cost, high-capacity backbone for global brain communication. Proc Natl Acad Sci U S A 2012;109:11372–7. https://doi.org/10.1073/pnas.1203593109.
[103] van den Heuvel MP, Sporns O. Network hubs in the human brain. Trends Cogn Sci 2013;17:683–96. https://doi.org/10.1016/j.tics.2013.09.012.
[104] Vázquez-Rodríguez B, Suárez LE, Markello RD, Shafiei G, Paquola C, Hagmann P, et al. Gradients of structure–function tethering across neocortex. Proc Natl Acad Sci 2019;116:21219–27. https://doi.org/10.1073/pnas.1903403116.
[105] Vij SG, Nomi JS, Dajani DR, Uddin LQ. Evolution of spatial and temporal features of functional brain networks across the lifespan. Neuroimage 2018;173:498–508. https://doi.org/10.1016/j.neuroimage.2018.02.066.
[106] Wen X, He H, Dong L, Chen J, Yang J, Guo H, et al. Alterations of local functional connectivity in lifespan: a resting-state fMRI study. Brain Behav 2020;10:e01652.
[107] Wu K, Taki Y, Sato K, Qi H, Kawashima R, Fukuda H. A longitudinal study of structural brain network changes with normal aging. Front Hum Neurosci 2013:7.
[108] Wu Z, Gao Y, Potter T, Benoit J, Shen J, Schulz PE, et al. Interactions between aging and Alzheimer's disease on structural brain networks. Front Aging Neurosci 2021:13.
[109] Yeh F-C, Panesar S, Barrios J, Fernandes D, Abhinav K, Meola A, et al. Automatic removal of false connections in diffusion MRI tractography using topology-informed pruning (TIP). Neurother J Am Soc Exp Neurother 2019;16:52–8. https://doi.org/10.1007/s13311-018-0663-y.
[110] Yeh F-C, Wedeen VJ, Tseng W-Y-I. Generalized q-sampling imaging. IEEE Trans Med Imaging 2010;29:1626–35. https://doi.org/10.1109/TMI.2010.2045126.
[111] Yeh F-C, Zaydan IM, Suski VR, Lacomis D, Richardson RM, Maroon JC, et al. Differential tractography as a track-based biomarker for neuronal injury. Neuroimage 2019;202:116131. https://doi.org/10.1016/j.neuroimage.2019.116131.
[112] Zamani Esfahlani F, Faskowitz J, Slack J, Mišić B, Betzel RF. Local structure-function relationships in human brain networks across the lifespan. Nat Commun 2022;13:2053. https://doi.org/10.1038/s41467-022-29770-y.
[113] Zhang Y, Brady M, Smith S. Segmentation of brain MR images through a hidden Markov random field model and the expectation-maximization algorithm. IEEE Trans Med Imaging 2001;20:45–57.
[114] Zhao T, Cao M, Niu H, Zuo X-N, Evans A, He Y, et al. Age-related changes in the topological organization of the white matter structural connectome across the human lifespan. Hum Brain Mapp 2015;36:3777–92. https://doi.org/10.1002/hbm.22877.
[115] Zhu W, Wen W, He Y, Xia A, Anstey KJ, Sachdev P. Changing topological patterns in normal aging using large-scale structural networks. Neurobiol Aging 2012;33:899–913. https://doi.org/10.1016/j.neurobiolaging.2010.06.022.
[116] Zimmermann J, Ritter P, Shen K, Rothmeier S, Schirner M, McIntosh AR. Structural architecture supports functional organization in the human aging brain at a regionwise and network level. Hum Brain Mapp 2016;37:2645–61. https://doi.org/10.1002/hbm.23200.
[117] Zonneveld HI, Pruim RH, Bos D, Vrooman HA, Muetzel RL, Hofman A, et al. Patterns of functional connectivity in an aging population: the Rotterdam Study. Neuroimage 2019;189:432–44. https://doi.org/10.1016/j.neuroimage.2019.01.041.
[118] Hinault T, Mijalkov M, Pereira JB, Volpe G, Bakke A, Courtney SM. Age-related differences in network structure and dynamic synchrony of cognitive control. Neuroimage 2021;236:118070. https://doi.org/10.1016/j.neuroimage.2021.118070.